

**GEOPHYSICAL INVESTIGATION FOR GROUNDWATER
IN THE TAIN DISTRICT OF THE BRONG AHAFO
REGION OF GHANA USING THE 2D CVES METHOD**

KNUST

BY

**Mohammed Mansuru Issah
B.Sc. Physics (Hons)**

**A Thesis Submitted to the Department of Physics,
Kwame Nkrumah University of Science and Technology
in partial fulfillment of the requirements for the degree
of**

**MASTER OF PHILOSOPHY
(GEOPHYSICS)**

College of Science

NOVEMBER, 2015

DECLARATION

I hereby declare that this submission is my own work towards the MSc and that, to the best of my knowledge, it contains no material previously published by another person nor material which has been accepted for the award of any other degree of the University, except where due acknowledgment has been made in text.

KNUST

Mohammed Mansuru Issah (PG 6151611)

Student Name & ID

Signature

Date

Certified by:

Dr. Akwasi Acheampong Aning

Supervisor Name

Signature

Date

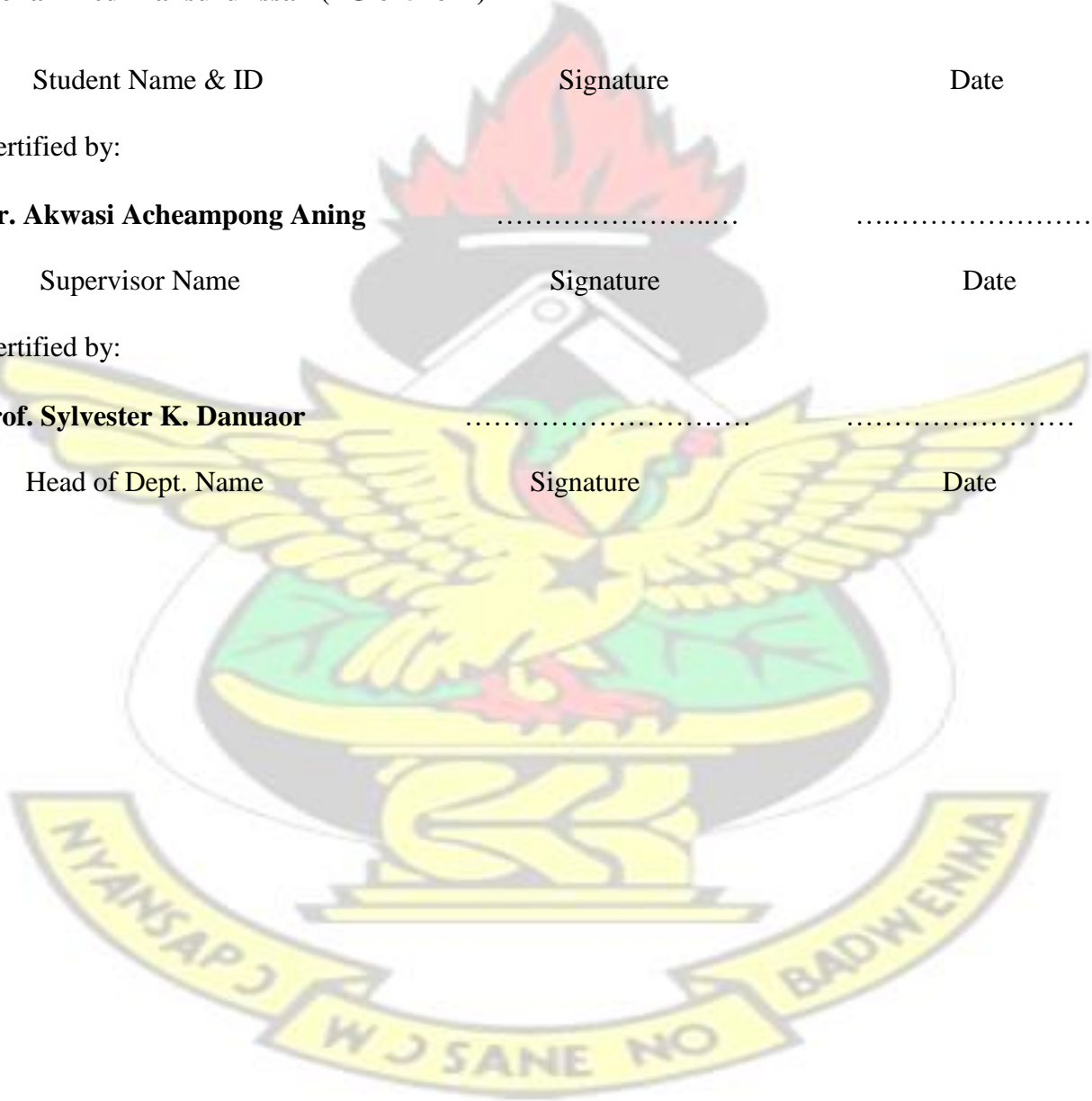
Certified by:

Prof. Sylvester K. Danuaor

Head of Dept. Name

Signature

Date



ABSTRACT

The 2D continuous vertical electrical sounding (2D CVES) surveys using the Wenner configuration were carried out in twenty communities in the Tain District. The objectives are to assess the subsurface geology, identify high groundwater potential zones in each community and the possibility of drilling high-yielding boreholes that could yield sustainable amount of groundwater for hand pump water supply. A total number twenty two 22 profiles were surveyed at least one in each community. The collected resistivity data was converted from the apparent resistivity data to 2D model section using the least-square inversion with the help of Res2Dinv software. The 2D resistivity model-section produced a high quality structural resolution leading to the demarcation of the layering of various lithological units, weathered layers and identification of important structures such as joints, fissures, fractures and faults. These structures are quite substantial in groundwater exploration. The study revealed that the potential water-bearing aquifer in the Tain district in the Black Volta Basin are mostly as a result of weathering of the overburden and fracturing of the underlying bedrock. The results of the study therefore suggest that the hydrogeology of the studied region is highly complex since the development of groundwater is generally due to secondary porosities. Based upon the results of the geophysical investigations, the groundwater potential zones in the twenty two communities were selected and expected to produce sufficiently high yielding boreholes enough for hand pump water supply system.

TABLE OF CONTENTS

CONTENTS	PAGE
DECLARATION.....	II
ABSTRACT	III
TABLE OF CONTENTS	IV
LIST OF FIGURES	VIII
ACKNOWLEDGEMENT	XI
1 INTRODUCTION	1
1.1 RESEARCH BACKGROUND	1
1.2 RESEARCH MOTIVATION	4
1.3 SCOPE OF THE WORK	5
1.4 OBJECTIVES	6
1.5 JUSTIFICATION	6
1.6 GROUNDWATER.....	7
1.6.1 GROUNDWATER OCCURRENCE	7
1.6.2 PERMEABILITY AND POROSITY	10
1.6.3 AQUIFERS	14

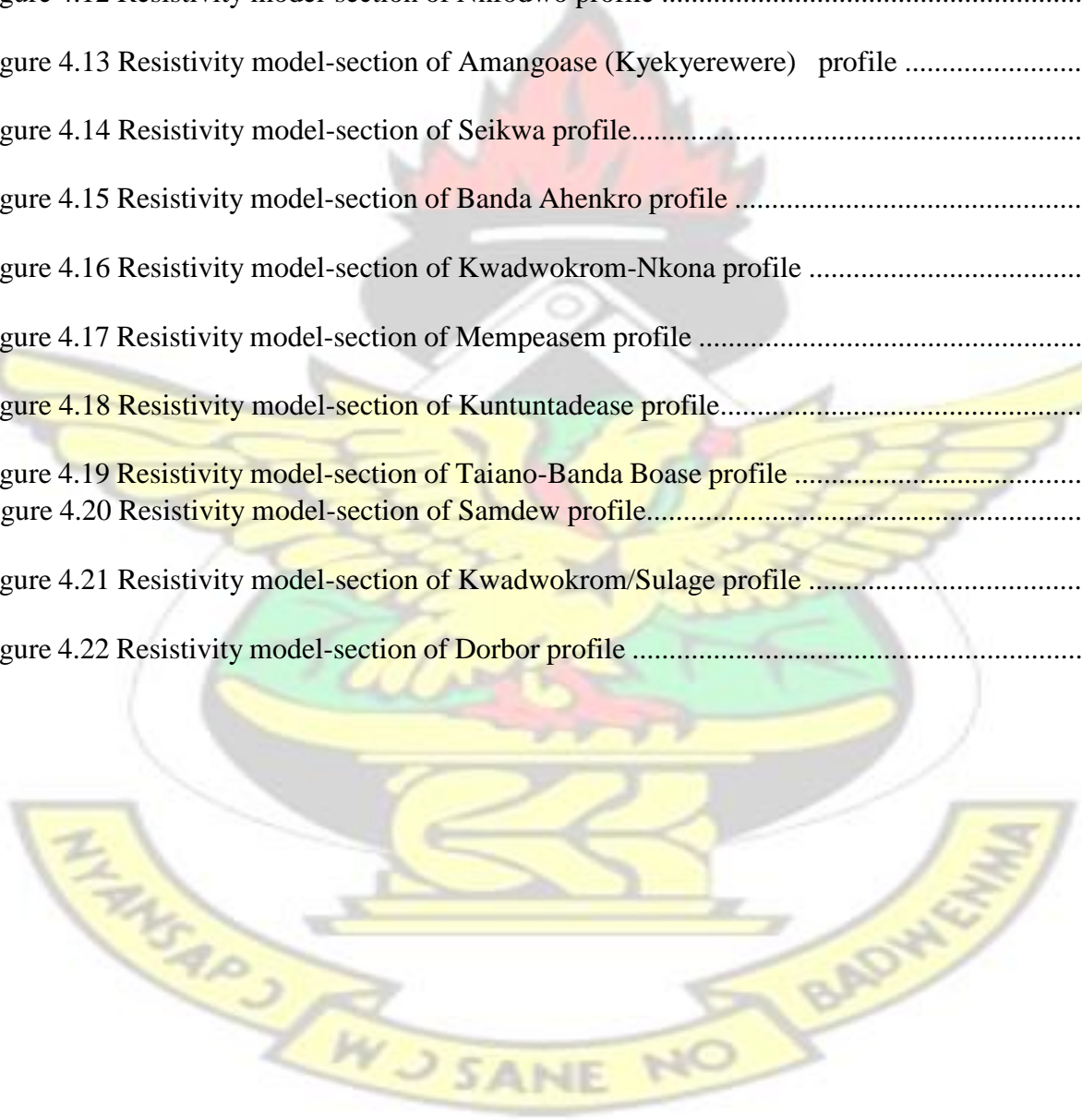
2	LITERATURE REVIEW	17
2.1	BASIC RESISTIVITY THEORY	20
2.1.1	INTRODUCTION	20
2.1.2	PRINCIPLES OF DC RESISTIVITY METHOD	21
2.1.3	ELECTRODE CONFIGURATION FOR RESISTIVITY SURVEY	27
2.1.4	FIELD PROCEDURE FOR RESISTIVITY SURVEY	30
2.1.5	2D MULTI-ELECTRODE ELECTRICAL RESISTIVITY IMAGING (ERI)	31
2.1.6	ELECTRICAL CONDUCTIVITY OF MINERALS AND ROCK MATERIALS	33
2.2	STUDY AREA	36
2.2.1	LOCATION AND DESCRIPTION OF THE STUDY AREA	36
2.2.2	GEOMORPHOLOGY AND CLIMATIC SETTING	37
2.2.3	WATER ACCESSIBILITY	37
2.2.4	GEOLOGICAL AND HYDROGEOLOGICAL BACKGROUND	40
3	METHODOLOGY	45
3.1	INTRODUCTION	45
3.2	DESK STUDY AND DATA COMPILATION	45
3.3	RECONNAISSANCE SURVEY	45
3.4	FIELD GEOPHYSICAL SURVEY	46
3.4.1	Introduction	46
3.4.2	The Field Procedure	47

3.4.3	Data processing	50
4	RESULT AND DISCUSSION	53
4.1	INTRODUCTION	53
4.2	ANALYSIS AND INTERPRETATION OF MODEL -SECTIONS	55
4.2.1	Menji profile A	55
4.2.2	Menji profile B	56
4.2.3	Kwametenten profile A	56
4.2.4	Kwametenten profile B	57
4.2.5	Debibi (Health Centre) profile	58
4.2.6	Sekogor profile.....	60
4.2.7	Ehiamankyene No. 2 profile	61
4.2.8	Wiasekrom profile	62
4.2.9	Mmaampehia profile	63
4.2.10	Bepoyease profile.....	64
4.2.11	Konkonti profile	65
4.2.12	Nnfodwo profile	66
4.2.13	Amangoase (Kyekyewere) profile	67
4.2.14	Seikwa profile	69
4.2.15	Banda Ahenkro profile	70
4.2.16	Kwadwokrom-Nkona profile	71

4.2.17	Mempeasem profile	72
4.2.18	Kuntuntadease profile	73
4.2.19	Taiano-Banda Boase profile	74
4.2.20	Samdew profile	75
4.2.21	Kwadwokrom/Sulage profile	76
4.2.22	Dorbor profile	77
5	CONCLUSION AND RECOMMENDATIONS.....	78
5.1	CONCLUSION	78
5.2	RECOMMENDATIONS	79
REFERENCES		
80		
APPENDIX		
87		
LIST OF FIGURES		
FIGURES		PAGE
Figure 1.1	The hydrologic cycle	8
Figure 1.2	Global distribution of groundwater resources	9
Figure 1.3	Types of aquifers.	16
Figure 2.1	Basic definition of resistivity across a homogeneous block	22
Figure 2.2	Current flowing radially away from the electrode so that the current distribution is uniform over hemispherical shells centered on the source.	23
Figure 2.3	The potential distribution caused by a pair of current electrodes	24
Figure 2.4	The generalised form of the electrode configuration used in resistivity measurements	

.....	25
Figure 2.5 The Wenner array	28
Figure 2.6 Schlumberger array	29
Figure 2.7 Dipole–dipole array	30
Figure 2.8 Schematic diagram showing the arrangement of electrodes for a 2-D electrical survey and the sequence of measurements for building up a pseudosection.....	32
Figure 2.9 Ranges of electrical resistivity for some common rocks, soil materials and minerals	35
Figure 2.10 Sources and nature of drinking water in the communities	38
Figure 2.11 (a) People waiting to fetch water (b) people traveling distance to access water facility.	39
Figure 2.12 Geological map of Ghana	43
Figure 2.13 Geological map of the Tain district	44
Figure 3.1 Profile line with jumpers connecting cable take-outs to steel electrodes	48
Figure 3.2 Set up of The ABEM LUND resistivity imaging equipment	49
Figure 3.3 Sketch of multi electrode array showing the set-up and a possible electrical resistivity tomography (ERT) model obtained after inversion	50
Figure 3.4 A sample of multiple electrode field data with some bad data points.	51
Figure 4.1 Resistivity model-section of Menji profile A	55
Figure 4.2 Resistivity model-section of Menji profile B	56
Figure 4.3 Resistivity model-section of Kwametenten profile A	57
Figure 4.4 Resistivity model-section of Kwametenten profile B	58
Figure 4.5 Resistivity model-section of Debibi (Heath centre) profile	59
Figure 4.6 Resistivity model-section of Sekogor profile	60

Figure 4.7 Resistivity model-section of Ehiamankyene No.2 profile	61
Figure 4.8 Resistivity model-section of Wiasekrom profile	62
Figure 4.9 Resistivity model-section of Mmaampehia profile	63
Figure 4.10 Resistivity model-section of Bepoyease profile	64
Figure 4.11 Resistivity model-section of Konkonti profile	65
Figure 4.12 Resistivity model-section of Nnfodwo profile	67
Figure 4.13 Resistivity model-section of Amangoase (Kyekyerewere) profile	68
Figure 4.14 Resistivity model-section of Seikwa profile.....	69
Figure 4.15 Resistivity model-section of Banda Ahenkro profile	70
Figure 4.16 Resistivity model-section of Kwadwokrom-Nkona profile	71
Figure 4.17 Resistivity model-section of Mempeasem profile	72
Figure 4.18 Resistivity model-section of Kuntuntadease profile.....	73
Figure 4.19 Resistivity model-section of Taiano-Banda Boase profile	74
Figure 4.20 Resistivity model-section of Samdew profile.....	75
Figure 4.21 Resistivity model-section of Kwadwokrom/Sulage profile	76
Figure 4.22 Resistivity model-section of Dorbor profile	77

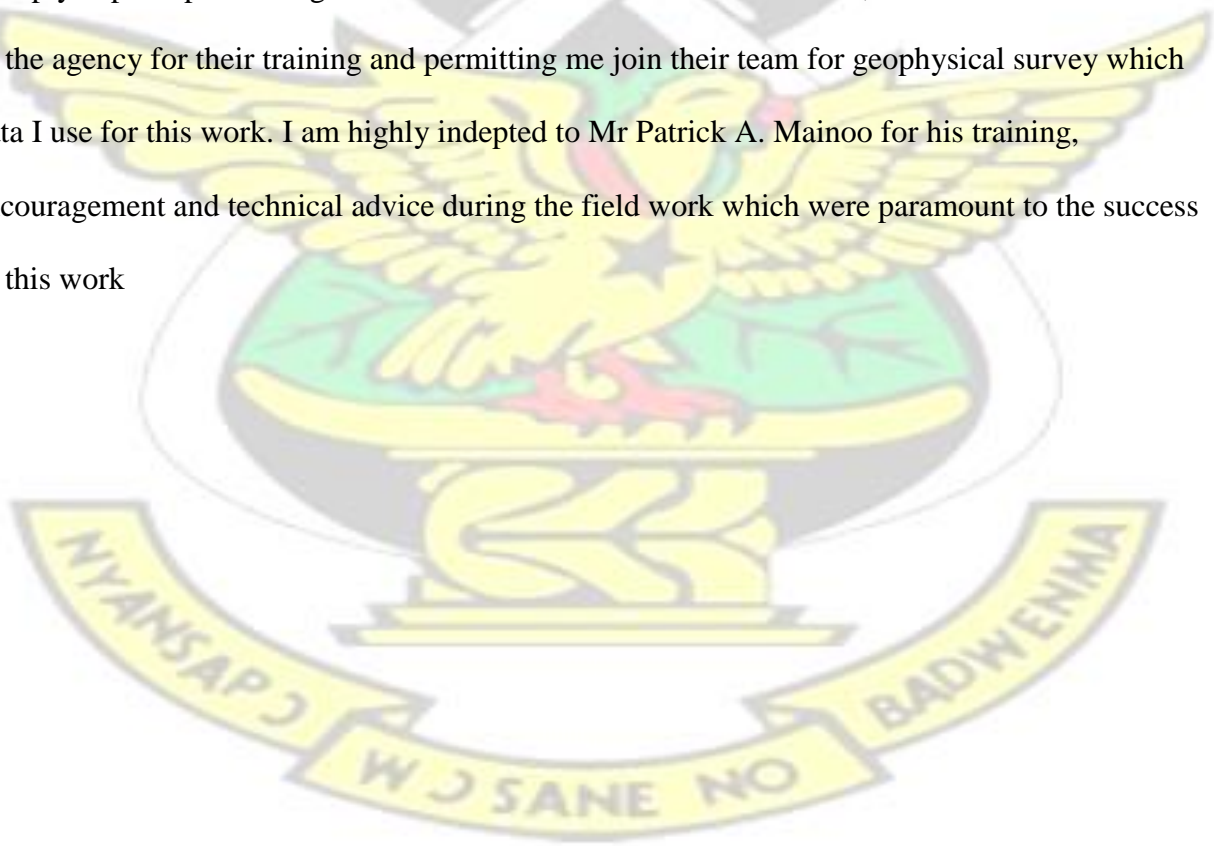


ACKNOWLEDGEMENT

My foremost gratitude and appreciation goes to the Almighty God for sustaining and seeing me through this MPhil programme.

I wish to express my profound gratitude and appreciation to my supervisor, Dr. A. A. Aning for all the selfless contributions, patience, constructive criticism and encouragement he made to see this work as a success. I am highly indebted to Head of Dept., Prof. S.K. Danuor and Dr. K. Preko for their unyielding support, guidance, encouragement and pieces of advice throughout my education. I am also grateful to all the geophysics lecturers at the Physics Department.

I deeply express profound gratitude to CSIR-Water Research Institute, Accra and the entire staff of the agency for their training and permitting me join their team for geophysical survey which data I use for this work. I am highly indebted to Mr Patrick A. Mainoo for his training, encouragement and technical advice during the field work which were paramount to the success of this work



CHAPTER ONE

1 INTRODUCTION

1.1 RESEARCH BACKGROUND

It has indisputably been said that water is life, and as everybody has the right to life, access to consumable water is a fundamental human right. Without it, we cannot survive, and there are no alternatives. As indicated by medical experts, water takes a more prominent share of the human body, and its vicinity helps keep the body in great shape. Water is part of the physiological process of nutrition and advised that it is a good thing for every human being to take at least eight glasses of water a day (WHO, 2004).

The accessibility or availability of potable water helps to reduce child mortality, as water-borne infections, for example, the guinea worm scourge would be radically diminished. In spite of water being basic necessity for life, many parts of the world, especially in developing countries including Ghana, sees it as a challenge to come across potable water. Most rural settlements have generally depended on various water from sources such as lakes, streams, dug-outs and impoundment repositories. Some of these surface water sources are intensely polluted, bringing about water-borne and water-related maladies, for example, diarrhoea, guinea worm, bilharzia, and so forth. (Gyau-Boakye *et al.*, 2008). The nature of drinking water is a compelling natural cause of wellbeing. Drinking water quality management has been a vital mainstay of essential counteractive action for waterborne infections for over 150 years; and it keeps on being the establishment of the avoidance and control of waterborne infections. Water is very important to life, however it can and does transmit infections in nations - from the deprived to the richest. The key leading

waterborne disease, diarrhoea, has a projected yearly frequency of 4.6 billion occurrences and causes 2.2 million deaths annually (WHO, 2010).

The accessibility of quality water has been the essential concern of rural communities in Ghana and all over Africa. The issue of acquiring a sufficient supply of potable water is becoming increasingly difficult as a result of increasing population which is resulting in increasing industrialization and agricultural activities. The shortage of water is not just unequivocal issue we are managing today, it has more future implications. Growth in the Economic and climate change is going to cause uncompromising scarcity and deprivation of global water resources and environments over the next 30 years, especial in the developing countries (Lloyd, 2010). The world is presently experiencing dry seasons in numerous parts of the world coupled with increasing population, particularly in the developing world. As surface supplies become extra worried because of increasing population which is resulting in increasing industrialization and agricultural activities, surface water becomes inadequate and undependable in supporting the growing human and animal population. Hence, there is the quest for other alternatives to supplement the surface water to sustain the request of the swelling population and industrialization activities. This makes the world to depend on one of the largest available source of quality fresh water which lies underground and this is referred to as groundwater. Subsurface openings large enough to yield water in a usable quantity to wells and springs underlie nearly every place on the land surface and thus make ground water one of the most widely available natural resources (Heath, 1987). Groundwater is extensively used as a source for drinking supply, domestic, irrigation and industrial purposes (UNESCO, 2004).

Although groundwater is a hidden resource, geophysical and geological principles can help specialists locate groundwater supplies and to delineate zones where no groundwater supplies are available.

Groundwater is contained and stored underneath the surface in rocks called aquifers. Groundwater sources are the largely reliable resource for use as drinking-water in most parts of the world, especially in areas with restricted or contaminated surface water sources. For some communities it might be the main economically reasonable choice. This is to some extent in light of the fact that groundwater is normally of more good condition and high contagious quality over surface waters. It needs almost no treatment to be proper for drinking although surface waters by and large must be treated (WHO, 2006).

Throughout Ghana, groundwater resource is important water supply mostly used for domestic water supply. About 70% of Ghana's population greatly depend on groundwater for drinking purposes (Kortatsi *et al.*, 2008) and the nature of groundwater asset is pivotal to giving the required requests to household, irrigation and industrial purposes (Anornul *et al.*, 2012). The provision of groundwater through modern hand-dug wells, boreholes, and piped systems has augmented considerably over the past years in the Volta River basin and hence groundwater has now become vital resource of water for urban and rural water source (Nicola *et al.*, 2005).

From an investigation carried conducted in Ghana by the Water Research Institute WRI of CSIR (1993) about 90 % of the rural and 25 % of the urban communities heavily rely on groundwater for their household water requests (Yankey *et al.*, 2011).

Groundwater flow is generally limited to fractures and joints in crystalline rock formations. Borehole yields are consequently frequently restricted (British Geological Survey, 2002). In region of thick layered regolith overlying the crystalline bedrock, there is potential expanded groundwater accumulation. Though this regolith is more typical in the range 1-70 m thick, the layer could be in abundance of 100 m thick in places (Asomaning, 1992 and British Geological Survey, 2002).

Due to the fact that greater number surface water supplies are unwholesome, the Ghana government has moved consideration from high cost of treatment of surface water to the development of groundwater to supply rural communities. Groundwater now shows a significant part in the socioeconomic growth of the country since the exploitation of groundwater for the water supply needs of several rural societies in the country has been on the rise over the last years.

The utilization of water for residential purposes cannot undoubtedly be recognized from beneficial use at the household level, especially among poor urban communities. Domestic water utilization to maintain livelihoods among the poor forms a fundamental piece of family adapting systems. There may likewise be paramount wellbeing and social gains from guaranteeing sufficient quality of service to help small-scale profitable usage utilization, for instance where this includes food production. Access to sufficient water for small-scale beneficial action in such regions is thus vital as a major aspect of poverty alleviation and may convey noteworthy health benefits accordingly (WHO, 2010).

1.2 RESEARCH MOTIVATION

Due to advancement in application of science and technology, geophysical methods have shown to be resourceful and cost-effective tools in groundwater exploration over the last three decades. Geophysics has not only been used for direct detection of the presence of water but also detection of the underground water level and thickness of aquifers, groundwater quality and movement, mapping saline water intrusions among others. Geophysics can provide additional data to improve the accuracy of groundwater models as a result of advances in microprocessors and related numerical models. These groundwater models are usually limited in precision by the

hydrogeological information obtainable. The ability to investigate the subsurface using geophysical techniques helps to identify potential drilling locations, hence, lessening the risk of drilling in unproductive areas.

Effectively, the cost of drilling large-scale water-supply boreholes for domestic and farming purposes in the study area requires that the risk of drilling a low-yielding and dry borehole is lessened through the appropriate usage of geophysical method. Therefore geophysical techniques always increase the success of drilling boreholes.

1.3 SCOPE OF THE WORK

The project involves geophysical investigations using electrical resistivity method to determine groundwater potential zones in twenty (20) communities within the Tain District of the Brong Ahafo Region of Ghana. The project work was carried out as part of TABCON CONSULT and WRI Ghana groundwater survey project of the Brong Ahafo Region. The work involved the use of continuous vertical electrical sounding (CVES) resistivity technique to identify potential groundwater sites in the communities which was then followed by drilling of the selected sites. The project work is therefore comprises geophysical field survey in the beneficiary communities in the study area, analysis and interpretation of the results.

1.4 OBJECTIVES

The objective of this project work is to carry out geophysical investigations in the project communities using continuous vertical electrical sounding (VES) resistivity technique to locate suitable sites (potential fresh water-bearing zones) for drilling of boreholes.

Specific objective:

- To delineate the depth and thickness of aquifer underlying each of the project communities.
- To locate fractures in subsurface rocks for borehole drilling.
- To map, locate and characterize all other subsurface features.

1.5 JUSTIFICATION

To effectively locate well sites, geophysical technique is essential in establishing the thickness of overburden and the depth to the underlying basement rocks, and further to detect the fractured areas of the bedrock (Erdelyi, 2010).

The use of the automated data acquisition system to produce 2D tomograms has greatly increased the rate and flexibility of electrical resistivity survey as a means for groundwater prospecting. Besides, the cost of carrying out resistivity survey and its interpretation is fast and straightforward. Resistivity technique is valuable in recognizing the various layers, variations and discontinuities within the layers of the subsurface because of its exceptional sensitivity to subsurface resistivity. These peculiarities and variations are generally very important regarding groundwater occurrence (Owen *et al.*, 2005).

2D electrical imaging surveys can provide useful results in various geological environment that are complementary to the information obtained by other geophysical methods (Loke, 2010). The interpretation leads to the knowledge of the maximum depth below which it would be likely for groundwater to occur. This is due to the fact that the resistivity of clean sand (not containing shale or silt) and gravel saturated with fresh water ranges between 20 and several hundred ohmmeter.

On the other hand, the resistivity of the same sand containing silt, clay or brackish water is much lower (Sabet, 1975).

KNUST

1.6 GROUNDWATER

1.6.1 GROUNDWATER OCCURRENCE

Groundwater is simply the kind of water that occurs under the earth surface in pore spaces between grains of mineral or in cracks and fractures in the rock mass. Groundwater hydrology is the branch of hydrological science that involves the application of the physical, biological, and mathematical principles in studying the occurrence, movement, and quality of water below the ground surface. Groundwater forms part of the hydrological cycle that describes the perpetual movement and occurrence of water between sea, atmosphere and land. It is an inconceivable, complex process driven by the sun's energy as shown in figure 1.1 (Heath, 1987).

Groundwater occurs in two different zones (Heath, 1987). The zone, which occurs just beneath the land surface in many regions containing both water and air and is known as the unsaturated zone or the zone of air circulation. This unsaturated zone is underlain by a zone in which all interconnected openings are filled with water and it is referred to as the saturated zone (Heath, 1987). The presence of groundwater as a water source depends to a large extent upon surface and subsurface geology and climate (Vandas *et al.*, 2002).

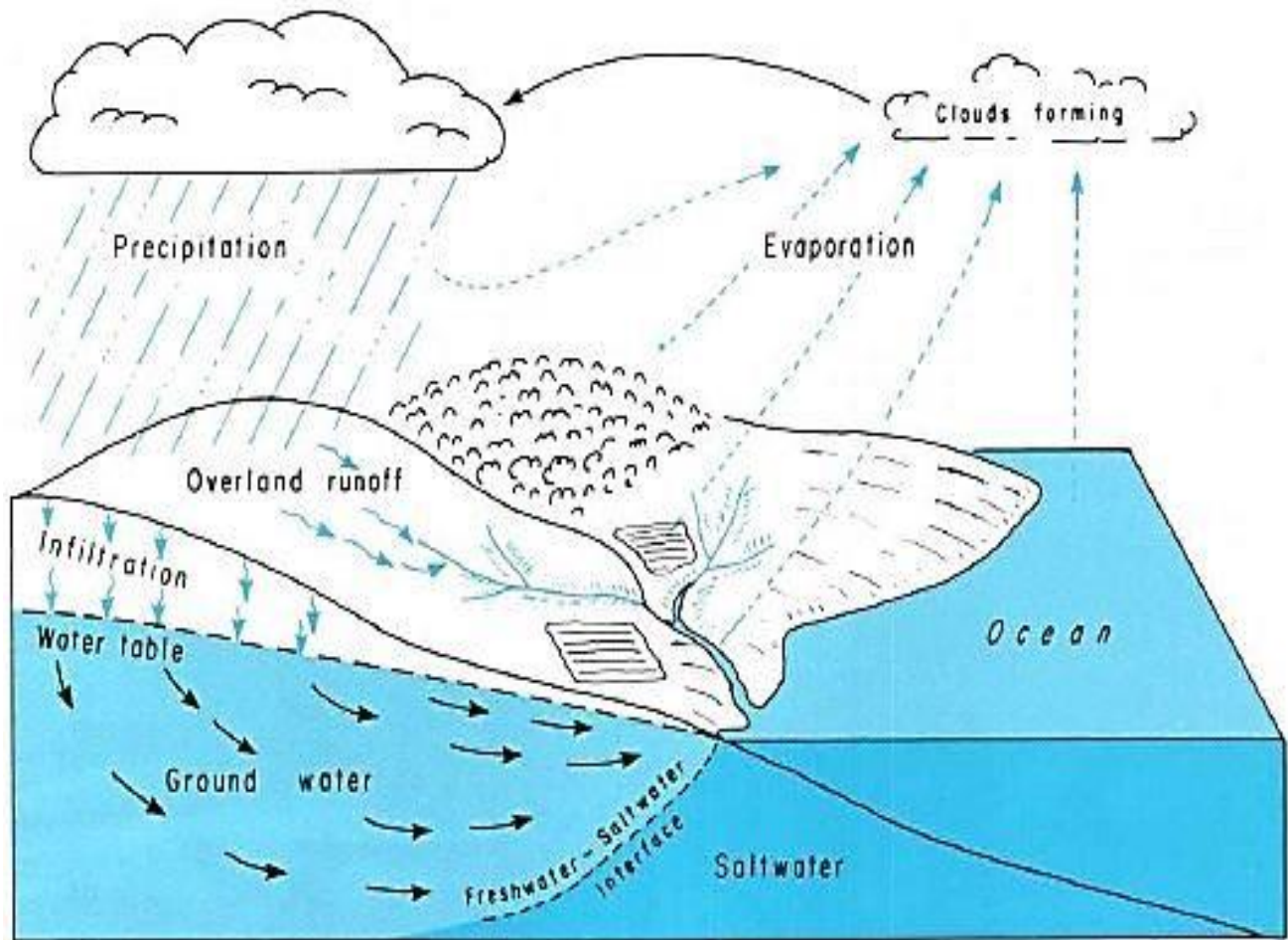


Figure 1.1 The hydrologic cycle (Heath, 1987)

The quantity of water that percolates into the ground will vary generally from place to place, fundamentally depending upon the topography of the area, the nature of the land surface and intensity and quantity of rainfall. The capability of a geologic formation to hold and transmit water is controlled by its porosity and penetrability. Therefore, in spite of abundant groundwater resources on a global scale, its distribution is uneven in both quantity and quality around the world (Figure 1.2) (WHYMAP, BGR and UNESCO, 2008).

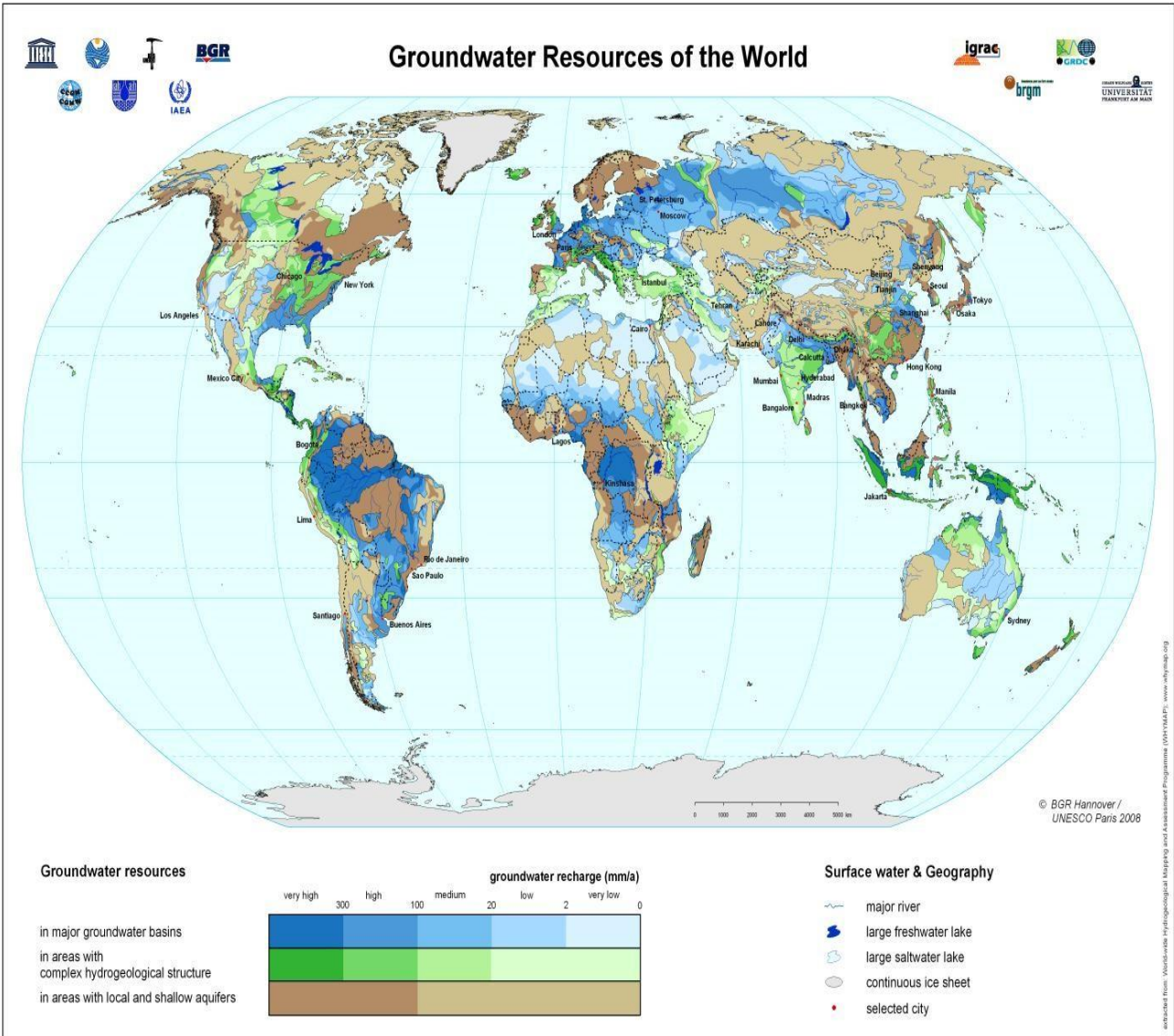


Figure 1.2 Global distribution of groundwater resources (WHYMAP, BGR and UNESCO, 2008)

1.6.2 PERMEABILITY AND POROSITY

1.6.2.1 Porosity

Porosity of rock is measured as a ratio of voids of rock material to the total volume of the rock.

Porosity of a rock therefore is a measure of its capacity to hold fluid. Porosity is extremely critical in groundwater hydrology since it gives us data on the maximum measure of water that a rock can

hold when it is saturated. In any case, it is similarly imperative to realize that only a part of this water is accessible to resource a well or a spring (Heath, 1987). The ratio of the volume of water that will drain under gravity from an initially saturated rock mass to the total volume of that rock is defined as the specific yield of the material, and is usually expressed as a percentage (Table 1.1).

Porosity is expressed quantitatively as

$$\phi = \frac{V_t - V_s}{V_t} = \frac{V_v}{V_t} \quad (1.1)$$

Where ϕ is the porosity of the rock sample, V_t is the total volume of soil or rock sample, V_s is the total volume of solids in the sample and V_v is the total volume of opening (void).

These open pore spaces occur between grains of sediments, in cracks or fractures and furthermore on a larger scale in deep openings created by disintegration of rocks. Porosity is classified as primary porosity or secondary porosity. Primary porosity is made up mainly of the spaces between grains, or inter-particle porosity, with some sediments also possessing intraparticle porosity formed by voids within grains, usually within the structures of shelly organisms. Primary porosity is the voids formed during the formation of the geologic material that is at the time of deposition. Cementation in sedimentary rocks reduces primary porosity because it reduces the voids. Secondary porosity develops after deposition and is an after effect of diagenetic processes: usually this happens as pore waters specifically dissolve parts of the rock such as shells made of calcium carbonate (Nichols, 2009).

Unconsolidated sands and rock are profoundly permeable with well-connected pore spaces making them probable high yielding aquifer. When grains forming the aquifer are about the identical size,

the pores containing water between the grains represent a bigger parcel of the aquifer volume compared with grains of varied size. Porosity of sedimentary rocks is largely influenced by the size and nature of grains the level of sorting and finally the degree of cementation. Sediments of coarse-grain normally have greater porosity than that of fine-grained due to the fact that the grains do not fit together well. The lower porosity of poorly-sorted sediments is mainly due to the fact that the fine-grained fragments have a tendency to fill in the open space. Highly-cemented sedimentary rocks have lower porosity on the grounds that cements have the tendency to fill in the pore space (Nelson, 2012). Porosity will decrease during the formation of clays and alteration products after deposition. Compaction and cementation after deposition will also reduce the absolute porosity. Generally, porosity decreases as depth increases. However, cementation is the principal process leading to porosity loss in sandstones (Barker Hughes INTEQ, 1999). Typical porosity and specific yield ranges for common geological materials are shown in Table: 1:1

Table 1.1 Porosity and specific yield of geological materials (UNESCO, WHO and UNEP, 1992; 1996; Freeze, 1979; Todd, 1980; Driscoll, 1986)

Material	Porosity (%)	Specific yield (%)
Unconsolidated sediments		
Gravel	25-35	15-30
Sand	25-45	10-30
Silt	35-50	5-10
Clay	45-55	1-5

Sand and gravel	20-30	10-20
Glacial till	20-30	5-15
<hr/>		
Consolidated rocks		
<hr/>		
Sandstone	5-30	3-15
Limestone and dolomite	1-20	0.5-10
Karst limestone	5-30	2-15
Shale	1-10	0.5-5
Vesicular basalt	10-40	5-15
Fractured basalt	5-30	2-10
Tuff	10-60	5-20
Fresh granite and gneiss	0.01-2	< 0.1
Weathered granite and gneiss	1-15	0.5-5

1.6.2.2 Permeability

Permeability of a rock is a measure of the ability of fluids to move through geologic formations. The unit of measurement is the Darcy, named after a French hydrologist who investigated flow of water through filter beds in order to design the public drinking fountains of the city of Dijon in the year 1856 (Bowen, 2008).

The permeability of a rock depends on its effective porosity; consequently, it is affected by the rock grain size, grain shape, grain size distribution (sorting), grain packing, and the degree of consolidation and cementation (Djebbar and Erle, 2004). Permeability can vary greatly depending on orientation (e.g. vertical permeability may be far lower than horizontal permeability) for the

same rock, especially if micas are abundant (WHO, 2006). It is conceivable to have profoundly porous rock with practically little or no interconnections between pores. A decent case of a rock with high porosity and low permeability is a vesicular volcanic rock, where the air pockets that once contained air give the rock a high porosity, however, since these openings are not linked with each other the rock has low permeability (Nelson, 2012). A thin layer of water may be pulled in to mineral grains because of the unsatisfied ionic charge on the surface. This is known as the molecular force of attraction. If the interconnections are not extensive, the water cannot move. Therefore, coarse-grained rocks are generally more porous than fine-grained rocks, and sands are more permeable than clays. (Nelson, 2012) . Permeability may also be strongly influenced by cross-bedding and other sedimentary structures (WHO, 2006).

For water to travel through an aquifer, the interior voids and fractures must be linked. Geologic formations with a high permeability could be the best aquifers and formations can have high porosity and not be good aquifers in the event that voids are not linked, or they are little. Cement development has the tendency to fill the pores of grains, leading to decreasing their permeability. Pore spaces could be totally filled by cement, bringing about a complete lithification of the sediment and to reduce its porosity and porousness to zero (Nichols, 2009).

Permeability in limestone is normally influenced by cracks and by openings brought about by water dissolving the rock. Most igneous rocks, such as granite, and metamorphic rocks, such as quartzite, have very low porosity and make poor aquifers unless they have interconnected fractures. Water travels through an aquifer from regions of recharge to zones of discharge. Recharge of groundwater happens from precipitation that infiltrates soils or that leaks from the bottom of surface water bodies, for example, lakes and streams (Vandas *et al.*, 2002).

1.6.3 AQUIFERS

An aquifer is a layer of a geologic formation or group of formations highly permeable and porous substrate that contains and transmits groundwater. When a unit of rock or an unconsolidated deposit can yield usable amount of water it is known as an aquifer. Sedimentary rock such as sandstone, as well as sand and gravel, are examples of good aquifers because they are water-bearing rock and therefore yield usable quantity of water. The upper level of this saturated layer of an unconfined aquifer is known as the water table.

The water table can be found at various depths anywhere between a few metres to several hundred metres below the earth's surface. The depth varies depending on geological setting and climate, lower in areas with high rainfall than in areas with low rainfall. When the amount of water flowing through the saturated zone changes, the depth to the water table may also change accordingly. The water table can increase in rainy season and drop in dry season. It is also important to mention that aquifers lie in between layers of impermeable rock such as sandstone, gravel, or fractured limestone or granite.

1.6.3.1 Types of aquifers

Aquifers are of two main categories (confined and unconfined aquifers) depending on the amount of water they contain and the degree of their inter-connections with different aquifers link to surface water (Kortatsi *et al.*, 2008).

1.6.3.1.1 Confined aquifers

Confined aquifers are permeable rock units deep under the ground between two layers of less permeable layers and filled with water, hence keep the free movement of air and water between the layers. Replenishment happens in areas known as recharge zones where the aquifer is unconfined and which may be a long distance from the confined portion of the aquifer (Kortatsi *et al.*, 2008). The water is hence kept under pressure and if tapped by a well rises to a level over the highest point of the aquifer, but not necessarily over the land surface. In the event that a well penetrates a confined aquifer, the hydraulic head or equilibrium elevation of the water level may be different from the confined elevation. The pressure may be so high that, water will naturally rise and flow freely to the surface without the need of a pump. This is called artesian flow. The water table in a confined aquifer is called the piezometric surface and does not necessarily follow the land surface. A perched aquifer represents a limited unconfined aquifer with an underlying confining layer that lies above and is differentiated from the local water table by an unsaturated zone.

1.6.3.1.2 Unconfined aquifers

Unconfined aquifers are characterised by the absence of a low-permeability layer above them yet have an aquitard only underneath. Their water tables are commonly close to the surface and generally follow the variation in the land surface. Because the water table, or the top of the saturated zone, marks the top of an unconfined aquifer, the thickness of the aquifer varies as the water table fluctuates with time (Kempton and Larson, 1997). These aquifers are essential wellspring of water due to their relative shallowness and their subsequent simple access. In lowlying regions, groundwater from these aquifers is regularly discharged as characteristic springs, streams and other surface water bodies. Figure 1.3 illustrates the various types of aquifers.

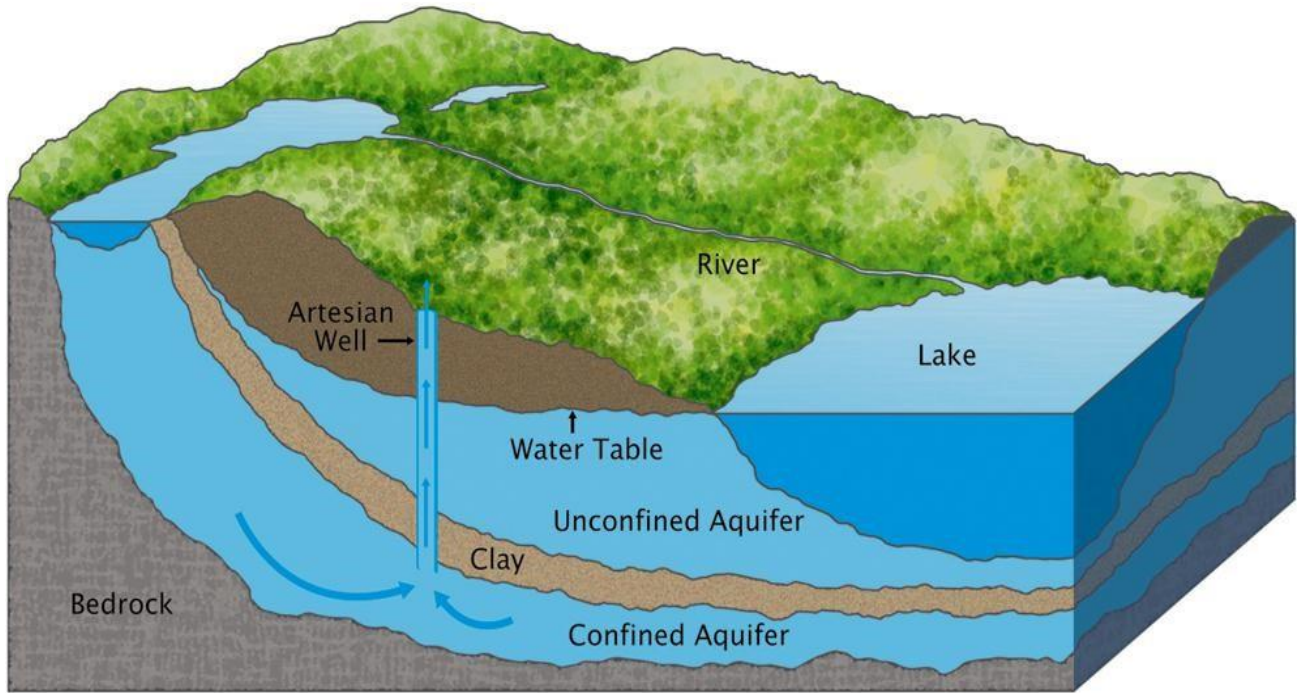


Figure 1.3 Types of aquifers (National geographic, 2013).

CHAPTER TWO

2 LITERATURE REVIEW

A wide range of geophysical surveying methods exists, for each of which there is an ‘operative’ physical property to which the method is sensitive. The type of physical property to which a method responds clearly determines its range of applications (Kearey *et al.*, 2002). For instance, the magnetic method is exceptionally suitable for locating buried magnetic bodies due to their high magnetic susceptibility. So also, seismic or electrical methods are suitable for the location of a buried water table in light of the fact that saturated rock may be distinguished from unsaturated rock by its higher seismic speed and higher electrical conductivity. In light of the relationship that

frequently exist between electrical properties, geologic formations and their fluid content, electrical and electromagnetic techniques can be employed in groundwater prospecting. The greater the porosity of the saturated rock, the lower its resistivity, and the higher the salinity of the saturating fluids, the lower the resistivity. The presence of clays and conductive minerals likewise lowers the resistivity of the rock (Zohdy *et al.*, 1974). Several geophysical surveys have been carried out in different parts of continents of the world for groundwater investigation.

Owen *et al.*, (2005), carried out a multi-electrode resistivity survey, over metasedimentary strata and metavolcanics in the Harare Greenstone Belt in north eastern Zimbabwe as part of a groundwater resources investigation. The resistivity results provided a clear view of the thickness of the weathered regolith and of the distribution of the various lithological units. The multi-electrode method is successful in identifying favourable zones for obtaining groundwater, such as areas with a maximum depth of weathered regolith, zones of fracturing and faulting, and high porosity and permeability zones associated with lithological contacts.

Bayewu *et al.*, (2012), conducted a study using VLF-EM and VES method to delineate fracture zones for groundwater exploration within the permanent site of Olabisi Onabanjo University, Ago-Iwoye, Southwestern Nigeria which is underlain mainly by suites of gneissic rocks. The basement fractures identified from VLF-EM anomaly curves were confirmed by geo-electric interpretation of the VES, therefore, the use of the two methods helped in the identification and delineation of promising prospective groundwater areas.

Ravindran *et al.*, (2012), carried out VES using Wenner electrode configuration with the help of equipment CRM 500 resistivity equipment to identify good sites in Teri deposits of Sawerpuram, Thoothukudi District, Tamil Nadu, India for groundwater exploration. In this rock types, groundwater occurs in secondary porosity developed due to weathering, faulting, fracturing in the

subsurface formation. The interpretations were carried out using apparent resistivity and SP logging techniques. The resistivity ranging from 100-120 Ωm indicated the freshwater zone in the study area.

Alile *et al.*, (2008), conducted geophysical study using VES, and employing the Schlumberger electrode configuration in a sedimentary environment to determine the suitability of the method for underground water studies. The VES data were obtained from two sites in Edo State, Nigeria. The high correlation between the VES results and the geologic section of a nearby borehole showed that the method is suitable for underground water exploration.

Ndlovu, (2011), carried out a study using two basic geophysical methods in groundwater exploration in the granite rock formation of Gwatemba area in southern Zimbabwe to identify high groundwater potential zones. The Slingram EM survey method was first used in line profiling which provided information of fractured, weathered, fissured and contact zones to a depth of approximately 30 m along the profile lines. VES using Schlumberger depth sounding technique was used at selected points which provided depth information below selected groundwater potential zones. The joint evaluation of the results provided both the lateral thickness and the depth of weathered part at a given point, which is the aquifer zone.

Van-Dycke and Menyeh (2013), conducted a study using resistivity profiling and VES to acquired data from some small communities and their surrounding areas within the Gushiegu and Karaga Districts of Northern Ghana, in order to study the aquifer characteristics and recommend hydro-geologically suitable sites to construct water supply boreholes for the communities. Interpretation of the resistivity profiling data resulted in the identification of weathered regions. The geoelectric sequence revealed predominantly three subsurface layer, which is largely congruous to the

weathering profile above the fresh bedrock - thick top soil, the weathered and the variably weathered and fractured bedrock respectively. The geophysical target is a reasonably thick and extensive zone of saturated weathered rock beneath the overburden. On the basis of the perceived aquifer properties, sites were recommended for drilling to supply water for the communities.

2.1 BASIC RESISTIVITY THEORY

2.1.1 INTRODUCTION

Geophysical resistivity and conductivity methods entails the studying of subsurface effects when electric current flows through the subsurface. Electrical resistivity methods are extensively used for investigating the shallow subsurface, particularly appropriate for resolving diverse environmental and hydrogeological problems. Either direct current (DC) or low frequency alternating current (AC) of about 20 Hz can be used for the investigation. The purpose of electrical survey is the investigation of variation in the subsurface electrical properties like the resistivity distribution. The subsurface resistivity variation can be correlated to geological parameters, for example, the minerals and amount of water, fracturing, porosity, conductivity of the saturate and the lithology. The technique is also valuable in recognizing the various layers, variations and discontinuities within the layers of the subsurface because of its exceptional sensitivity to subsurface resistivity. These peculiarities and variations are generally very important regarding groundwater occurrence (Owen *et al.*, 2005).

The occurrence of water controls a significant part of variation of the ground resistivity. The degree of water saturation and network of opening space gives an estimation of the subsurface resistivity. This is due to the fact that water highly conductive and hence less resistive and current will move through regions of low resistance. Increase in salinity of ground water, increase saturation, increase porosity and degree of fracturing of rock, each of these has the tendency to reduce resistivity. Increase in the degree of compaction within the lithology reduces the amount water and eventually increases the resistivity. The occurrence of water decreases resistivity while the vicinity of pore air raises resistivity since air unsurprisingly has pronounced resistivity.

In the light of the fact that, the passage of current in the near surface is as a result of the movement of ions with the pore space, porosity is the real controlling component for variation in resistivity. It is very tedious in estimating resistive anomalies than conductive anomalies, since the majority of minerals are non-conductive and rock structure has a tendency to affect resistivity (Cardimona, 2008).

2.1.2 PRINCIPLES OF DC RESISTIVITY METHOD

The majority of minerals forming rock are extremely non-conductive, and the passage electric current through is mainly ionic pore water. The vicinity and the degree of the dissolved ions in pore water determines their conductivity since pure water is less ionised (Milsom, 2003).

The electrical properties of a material is described by Ohm's law

$$V = I \times R \quad \therefore R = \frac{V}{I} \quad (2.1)$$

The constant of proportionality R , the resistance and the unit is ohm (Ω). The reciprocal, conductance, is measured in Siemens.

The above relationship holds for earth materials. Resistance R , however, is not a material constant. It rests not only on the material of the medium, but also depends on its geometry. It is well known that the resistance R , in ohms, of a wire is directly proportional to its length L and is inversely proportional to its cross-sectional area A . That is

$$R = \rho \frac{L}{A} \quad (2.2)$$

Resistivity ρ is a fundamental property of the medium relating the resistance of the medium to the flow of electric current. The resistivity ρ of a material is defined as the resistance in ohms between the opposite faces of a unit cube of the material through which the current is passing (Milsom, 2003).

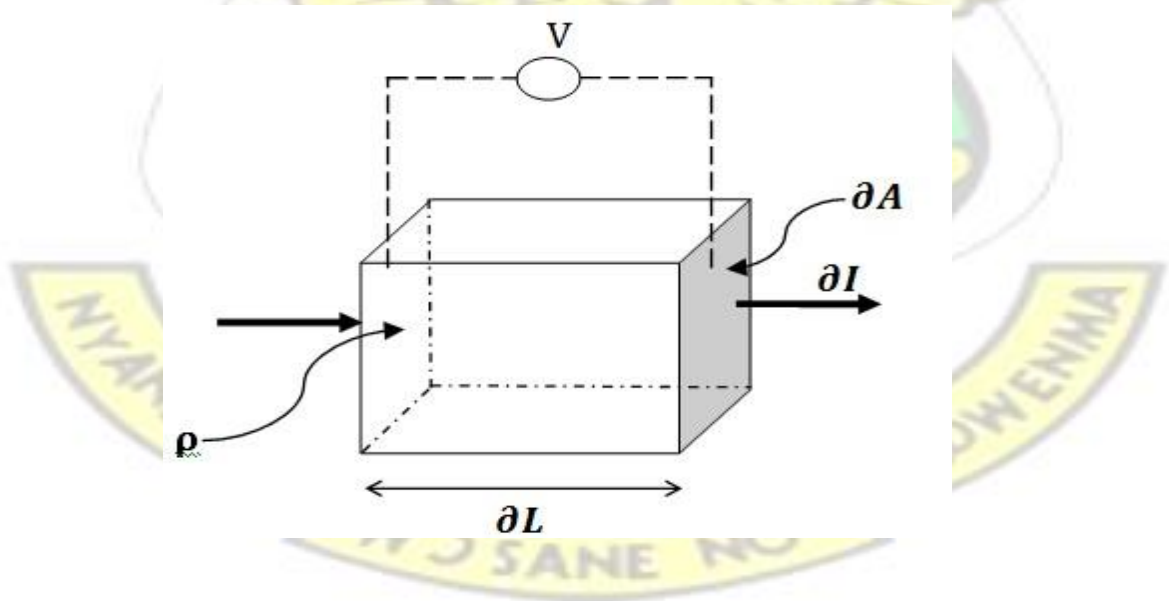


Figure 2.1 Basic definition of resistivity across a homogeneous block

For a conducting block (Figure 2.1) of resistance R , length L and cross sectional area A , the resistivity ρ is given by

$$\rho = \partial R \cdot \frac{\partial A}{\partial L} \quad (2.3a)$$

$$\rho = \frac{V}{I} \cdot \frac{A}{L} \quad (2.3b)$$

The current density at any point in the medium is defined as the amount of current passing through a unit area of an equipotential surface. The current density J is related to electric field strength E through the ohm's law by the expression.

$$J = \sigma E = \sigma \nabla V \quad (2.4)$$

Where $\sigma = 1/\rho$

$$J = \frac{1}{\rho} E \quad (2.5)$$

$$J = \frac{I}{A} = \frac{\nabla V}{\rho L} \quad (2.6)$$

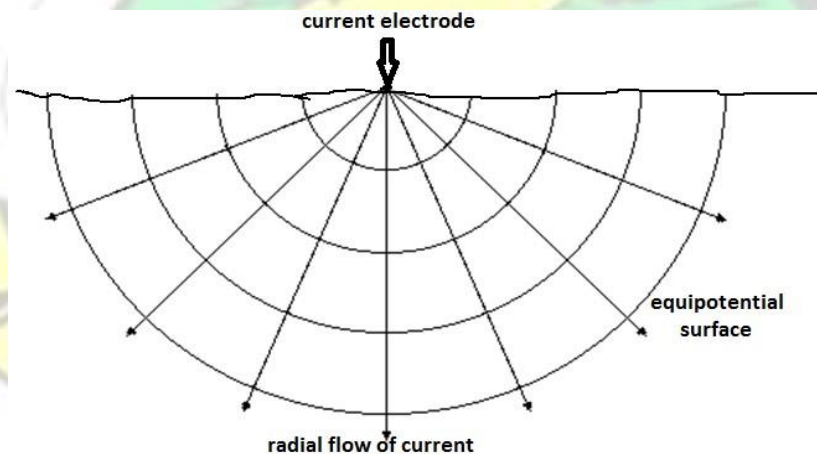


Figure 2.2 Current flowing radially away from the electrode so that the current distribution is uniform over hemispherical shells centered on the source.

The current density decreases with increasing distance from the current source due to the current flowing radially away from the electrode. Hence the current distribution is uniform over hemispherical shells centered on the source. It is possible to calculate the voltage at a distance (r) from a single current point source as shown in figure 2.2

$$J = \frac{I}{\frac{1}{2}(4\pi r^2)} = -\frac{1}{\rho} \frac{dV}{dr} \quad (2.7)$$

The equation (2.8) gives the fundamental theoretical study of the current flow in subsurface for the case of a homogeneous isotropic subsurface with a single current electrode on the ground surface. The current flows radially away from the source, and the potential varies inversely with separation from the current source. The electric potential V at any point caused by a point electrode producing current I in an infinite homogeneous and isotropic medium of resistivity ρ is given by

$$V(r) = \frac{I\rho}{2\pi r} \quad (2.8)$$

Practically, very resistivity studies use at least a pair current electrodes and a pair of potential electrodes (Loke, 1997). The potential values have a symmetrical pattern about the vertical plane at the mid-point between the two electrodes (figure 2.3).

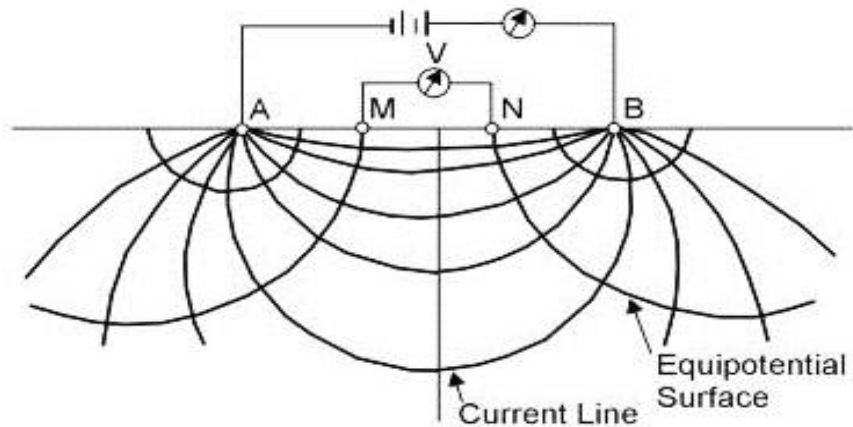


Figure 2.3 The potential distribution caused by a pair of current electrodes (U. S. Environmental Protection Agency, 2011)

Consider an arrangement consisting of two potential electrodes M and N and two current electrodes, A and B (Figure 2.4). The current electrodes A and B act as source and sink, respectively. In this case there are two points (potential electrodes positions) where we need to find the electric potentials due to the source (current electrode, A) and also due to the sink (current electrode, B) and hence obtain the potential difference between the two points.

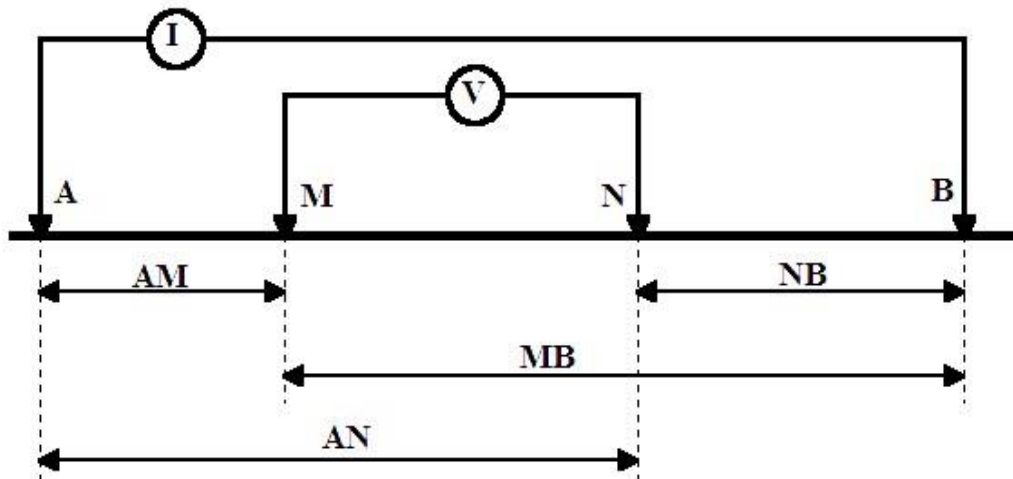


Figure 2.4 The generalised form of the electrode configuration used in resistivity measurements

The electrode, M is at distances AM and MB from the source and sink, and the electrode, N is at a distance of AN and NB. The potential V_M measured at electrode M is given by

$$V_M = \frac{I\rho}{2\pi} \left(\frac{1}{AM} - \frac{1}{MB} \right) \quad (2.9a)$$

The potential V_N measured at electrode N is given by

$$V_N = \frac{I\rho}{2\pi} \left(\frac{1}{AN} - \frac{1}{NB} \right) \quad (2.9b)$$

The total potential difference between the electrode M and N is given by the expression

$$\Delta V = V_M - V_N \quad (2.10)$$

$$\Delta V = \frac{I\rho}{2\pi} \left[\left(\frac{1}{AM} - \frac{1}{MB} \right) - \left(\frac{1}{AN} - \frac{1}{NB} \right) \right] \quad (2.11)$$

For arrays, the potential at any potential electrode is equal to the sum of the contributions from the individual current electrodes. The resistivity in a four-electrode survey over homogeneous ground is found by rearranging equation(2.11).

Therefore, the resistivity of the half-space is thus given by

$$\rho = \frac{\Delta V}{I} K \quad (2.12)$$

Where

$$K = 2\pi \left[\left(\frac{1}{AM} - \frac{1}{MB} \right) - \left(\frac{1}{AN} - \frac{1}{NB} \right) \right]^{-1} \quad (2.13)$$

K is called the geometric factor which depends on the specific positions of current and potential electrodes.

Because the sub-surface is as matter of fact heterogeneous in nature, the resistivity attained is not the true resistivity but rather the apparent resistivity (ρ_a) which can even be negative. It is very important to remember that the resistivity values measured on the field is not true resistivity of the sub-surface but apparent resistivity. Whereas resistivity values acquired by interpretation are 'true' resistivities (Reynolds, 1997).

2.1.3 ELECTRODE CONFIGURATION FOR RESISTIVITY SURVEY

Generally, the four electrodes A, B, M and N (Figure 2.4) can be placed at arbitrary positions on the ground. An exception to this is the Lee Partition electrode array, which uses five (5) electrodes (Amarachi and Ako, 2012). Each electrode configuration offers advantages in equipment handling or in measurement instrumentation. Despite the fact that various diverse arrangements have been offered for the resistivity studies, the generally utilized designs are the Schlumberger, Wenner, and dipole-dipole configurations. For all the arrays, the four electrodes are collinearly arranged but with distinctive electrode separation and geometries are different (Lowrie, 2007). The geometry of the electrode of a configuration determines the apparent resistivity measured by the array. The value of apparent resistivity ρ_a depends on the four distance-variables AM, AN, BM, and BN (Zohdy *et al.*,1974).

2.1.3.1 Wenner Configuration

The Wenner configuration is the simplest in that current and potential electrodes are kept at an equal spacing a (Kearey, 2002) (Figure 2.4). The Wenner array consists of four collinear, equally-spaced electrodes. The outer two electrodes are typically the current electrodes and the inner two

electrodes are the potential electrodes. In the Wenner array, the electrode spacing expands about the array midpoint while maintaining an equivalent spacing between each electrode. The apparent resistivity, ρ_a , for the Wenner configuration is given by the following expression

$$\rho_a = 2\pi a \frac{\Delta V}{I} \tag{2.14}$$

With this configuration, apparent resistivity can effectively be computed in the field and the equipment sensitivity is not as essential compared with other array geometries. Generally little current is required to produce measurable potential difference. The disadvantage is that all the electrodes would have to reposition for each sounding.

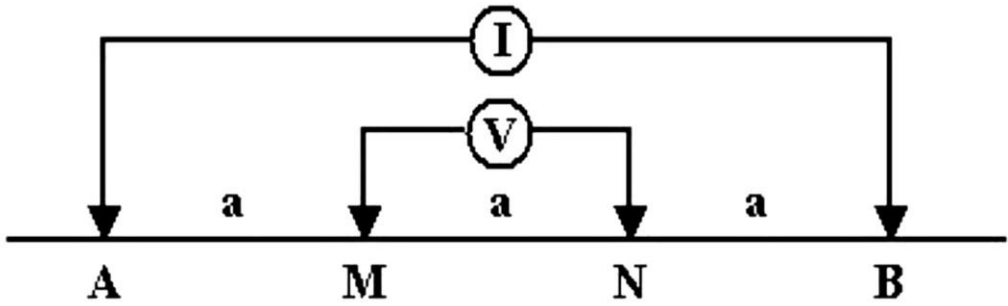


Figure 2.5 The Wenner array

2.1.3.2 Schlumberger configuration

This array is the most widely used in electrical prospecting (Zohdy *et al.*, 1974). The Schlumberger array made up of four collinear electrodes with the outer two electrodes A and B being the current electrodes whereas the inner two electrodes M and N, the potential electrodes (Figure 2.6). With this configuration, the potential electrodes are kept at the center at a separation usually less than one fifth of the separation between the current electrodes. The potential electrodes are kept constant whereas the current electrodes are increased. The potential electrode spacing is assumed

to be infinitesimal, and the observed value of potential can be adjusted accordingly (Dobrin and Savit, 1988). The apparent resistivity, ρ_a , for Schlumberger configuration is given by the following expression

$$\rho_a = \frac{\pi}{a} \left(s^2 - \left(\frac{a}{2} \right)^2 \right) \frac{\Delta V}{I} \tag{2.15}$$

With the Schlumberger configuration, less electrodes are relocated for each sounding. Substantially, Schlumberger sounding has very good resolution and better depth of penetration, and easy field deployment. The disadvantages are that long current electrode cables are required.

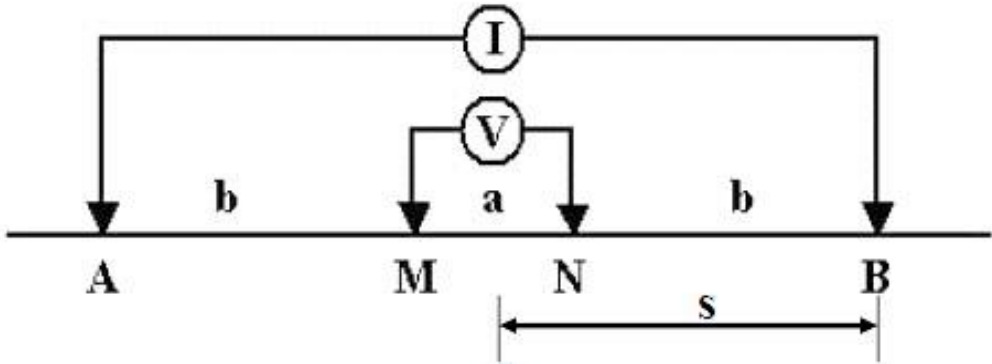


Figure 2.6 Schlumberger array

2.1.3.3 Dipole-dipole Configuration

The dipole-dipole electrode array consists of two sets of electrodes, the current set and potential set electrodes. A dipole is a paired electrode set with the electrodes located relatively close to one another. The dipole-dipole electrode arrangement is illustrated in (figure 2.7). The convention for a dipole-dipole electrode array is to maintain an equal distance for both the current and the potential electrodes (spacing = *a*), with the distance between the current and potential electrodes

as an integer multiple of a . The electrodes do not need to be located along a common survey line. The apparent resistivity, ρ_a , for dipole-dipole configuration is given by the following expression

$$\rho_a = 2\pi n(n + 1)(n + 2)a \frac{\Delta V}{I} \quad (2.16)$$

The main advantage of the dipole-dipole electrode array is that, it is easy to deploy in the field due to shorter wire lengths. However, a large generator may be needed to transmit a greater current magnitude for the measurement, especially for deep soundings.

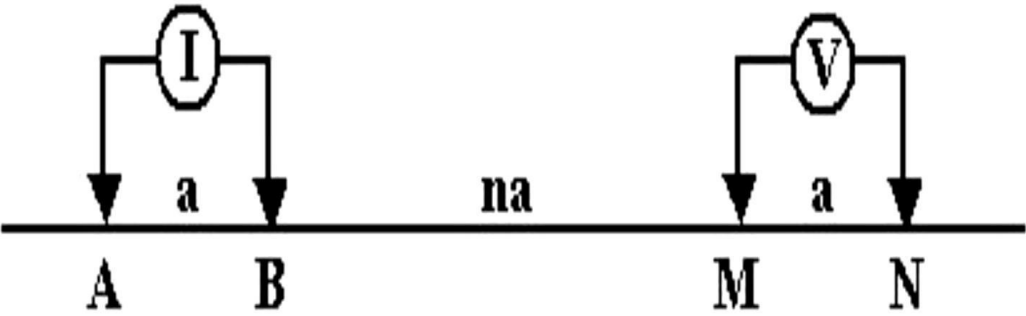


Figure 2.7 Dipole–dipole array

2.1.4 FIELD PROCEDURE FOR RESISTIVITY SURVEY

There are two (2) main basic procedures employed in resistivity method and these are vertical electrical sounding (VES) and constant separation traversing (CST) which is also known as electrical profiling. The specific technique to be employed depends on whether one is interested in the variation of resistivity with depth or variation of resistivity with lateral extent.

2.1.4.1 Vertical electrical sounding (VES)

VES is used to variation in resistivity with depth. The electrode separation is varied for every measurement, but the centre point of the array is kept constant. The technique is widely utilised in

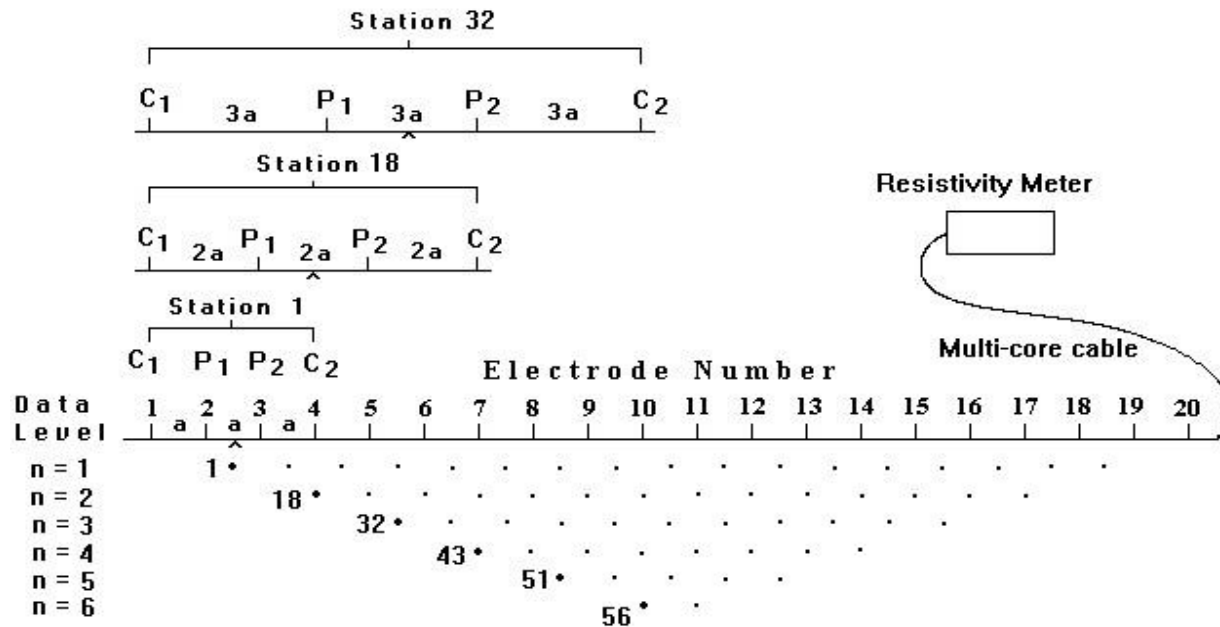
geotechnical investigations to establish overburden thickness and in hydrogeology to define horizontal zones of porous strata.

2.1.4.2 Constant separation traversing (CST)

CST is used to determine the lateral variations in resistivity. In this arrangement, the electrode separation is fixed while the centre of the array is varied. In the profiling technique, only variation and discontinuity in resistivity with lateral extensions of the subsurface are recognised as anomalies beneath the profiles.

2.1.5 2D MULTI-ELECTRODE ELECTRICAL RESISTIVITY IMAGING (ERI)

Unlike the conventional techniques, the profiling method, where only variation in resistivity with lateral extensions of the subsurface are recognised as anomalies beneath the profiles; and sounding (VES), where only variation and discontinuity in resistivity with depth are recognised as anomalies beneath the profiles. ERI simultaneously studies both vertical and lateral distribution of resistivity beneath the whole profile. This particular resistivity technique helps to detect water-bearing zones between two points of survey. The two dimensional (2D) data generated using multi-electrodes results in high density pseudo-sections with dense sampling of apparent resistivity measurements at shallow depth ranging from surface to a depth of 300 m in a short time (Dewashish, 2012). The ERI method is comprehensively used in groundwater exploitation, environmental and geotechnical studies (Ratnakumari *et al.*, 2012).



Sequence of measurements to build up a pseudosection

Figure 2.8 Schematic diagram showing the arrangement of electrodes for a 2-D electrical survey and the sequence of measurements for building up a pseudosection (Loke, 2010)

ERI is mostly carried out using a large number of equally spaced collinear array of electrodes connected to a multi-core cable. The separation between the potential electrode and the current electrodes depends on the electrode configuration. A laptop computer coupled with an electronic switching unit is used to automatically select the relevant electrodes to be used as potential electrode pair and current electrode pair for each measurement. Figure 2.8 illustrates a potential arrangement of measurements for the Wenner electrode configuration for a system with 20 electrodes.

The apparent resistivity measurements are normally presented in a graphical form using the model sections (Figure 3.3) which gives approximate section of the subsurface resistivity distributions.

2.1.6 ELECTRICAL CONDUCTIVITY OF MINERALS AND ROCK MATERIALS

Electrical resistivity or conductivity and permittivity are the essential basic characteristic of rock that numerous geophysical methods depend on (Lowrie, 2007). When an electric field is applied, electrical current flows in materials because of the movement of charged particles (electrons and/or ions). The electrical conductivity (σ) of a material is a measure of how easy or difficulty with which an electrical current can be made to flow through it. With exception of graphite, metallic minerals and some clay, most soil materials are poor conductors and any current that flows in these soils is mostly because of the pore water and its ionic content.

The means of conduction of current within rocks are dielectric conduction, electronic and electrolytic (Reynolds, 1997). Electrolytic conduction is comparatively gentle passage of ions through electrolyte and relies on the kind of ion, mobility, concentration, etc. Electronic conduction is rapid passage of electrons (charges) through metallic materials. Dielectric conduction is the passage current through insulators by the application of an external alternating current (Reynolds, 1997).

Unconsolidated sediments and most mineral rocks of the Earth crust are principally made up of silicate, which are electrical insulators. The current in these materials is carried by ions in the pore solutions and hence the conductivity of these rocks is mainly due to the amount of water contained in their pores. The conduction current through porous rock depends on the bulk and composition of the pores and the measure of the water in the pores. The net resistivity of a rock formation which takes into account the porosity can be expressed in terms of the resistivity and volume of the pore water present according to an empirical formula given by Archie (1942).

$$\rho = a \Phi^{-m} S^{-n} \rho_w = \frac{a}{\Phi^m S^n} \rho_w \quad (2.17)$$

Where Φ is the fractional pore volume (porosity), S the fraction of pores holding water of resistivity ρ_w and a , m and n are empirical constants. Where $n \approx 2$ $0.5 \leq a \leq 2.5$, $1.3 \leq m \leq 2.5$

(Telford *et al.*, 1990).

$$\frac{\rho}{\rho_w} = a \Phi^{-m} S^{-n} = \frac{a}{\Phi^m S^n} = F \quad (2.18)$$

The ratio ρ/ρ_w is known as the formation factor (F), ρ_w can differ significantly depending on the quantities and the ability of dissolved materials to conduct. Archie's law is used predominantly in borehole logging (Reynolds, 1997). The range of resistivities among rocks is large, extending from under 10^{-2} to $10^8 \Omega\text{m}$ and above.

Rocks and minerals with resistivities below $1.0 \Omega\text{m}$ are considered good conductor; those from 1 to $100 \Omega\text{m}$, intermediate conductor; and those greater than $100 \Omega\text{m}$, poor conductors (Zohdy *et al.*, 1974). Figure 2.9 displays expected wide range of resistivities for common types of rock, soil materials and minerals.

The resistivity values of igneous and metamorphic rocks are naturally very high. The level of fracturing, and the fraction of the fractures containing water are the factors that significantly influence resistivity igneous and metamorphic rocks. The level of fracturing, and the fraction of the fractures containing water are the factors that significantly influence resistivity igneous and metamorphic rocks. Depending on level dryness or wetness, such rocks may have a wide range of resistivity of about (1000 - 10 million) Ωm

This characteristic is valuable in detecting fractures and weathering features, for example, in engineering and groundwater studies (Loke, 2010).

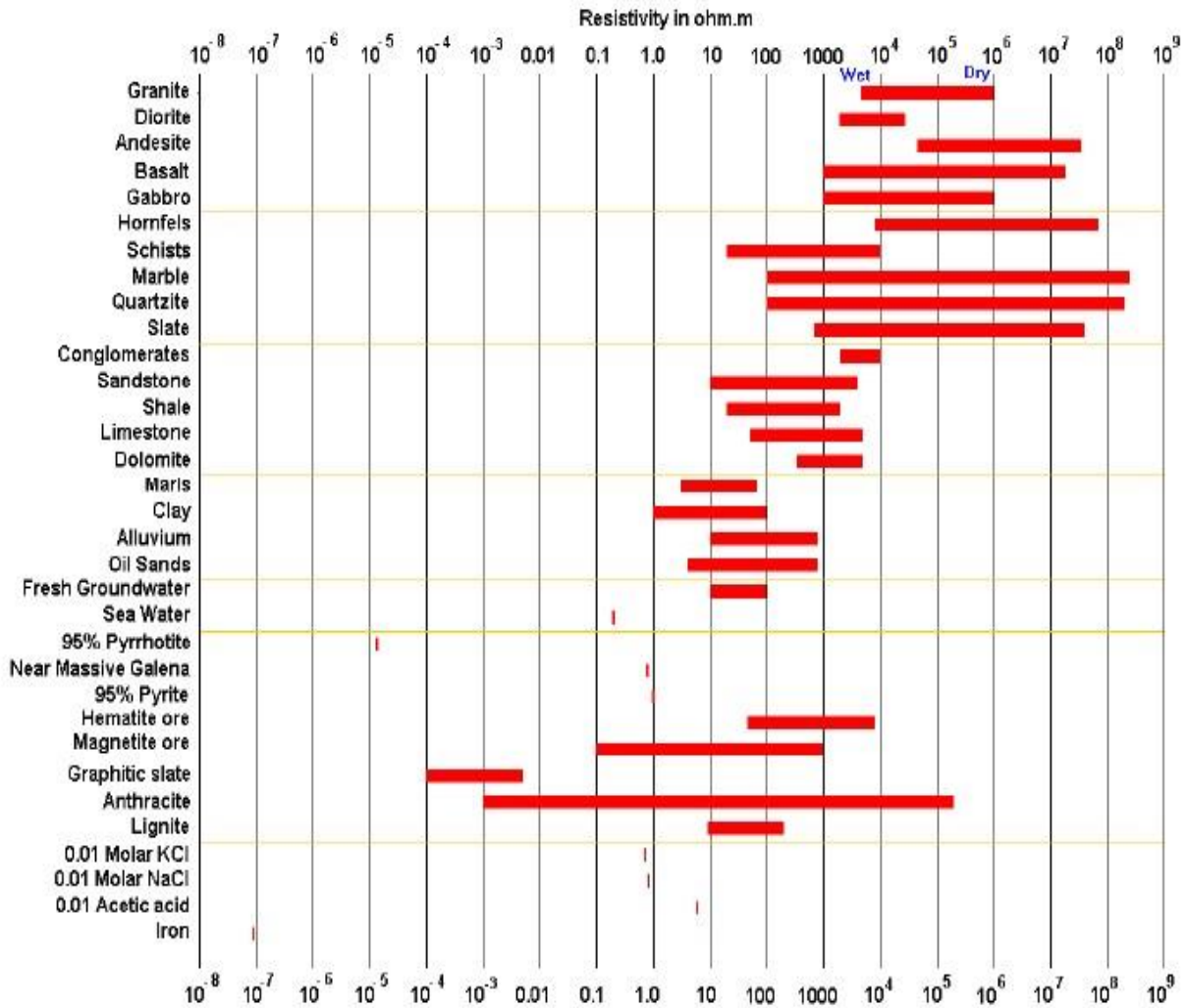


Figure 2.9 Ranges of electrical resistivity for some common rocks, soil materials and minerals (Loke, 2010)

The resistivity values of sedimentary rocks ranges from 10 to about 10,000 Ωm , but most resistivity values falls below 1000 Ωm (Loke, 2010). The low resistivity values are due to the fact that sedimentary rocks have high porosity and contains higher amount water. The resistivity of the interstitial fluid in sedimentary rocks is more important than that of the host rock.

The resistivity value of unconsolidated sediments ranges from about 10 to less than 1000 Ωm (Loke, 2010). Sedimentary rocks mostly have greater resistivity values than unconsolidated sediments and the resistivity value is subject to the porosity in addition to clay content.

Base on the concentration of dissolved salts, the resistivity of groundwater diverges from 10 to 100 Ωm (Loke, 2010). Saline groundwater may have a resistivity as low as 0.05 Ωm and some groundwater and glacial melt water can have resistivities in excess of 10000 Ωm (Reynolds, 1997).

2.2 STUDY AREA

2.2.1 LOCATION AND DESCRIPTION OF THE STUDY AREA

The Tain District is located at North West of Sunyani. It lies within latitudes 7.555 N and 8.204 N North and longitudes 2.007 West and 2.784 West. In terms of land area, Tain District covers 4,125km². Nsawkaw, the district capital is 29 km from Wenchi, the capital of Wenchi Municipal which Tain was carved out in 2004. The district shares common boundaries with Jaman North to the west, Wenchi Municipal to the east, Sunyani Municipal to the south and Berekum Municipal to the south-west. It is also bounded by the Bole District of the Northern Region to the north east and La Cote d'Ivoire to the north-west (Tain District Assembly, 2006).

Availability of potable water supply is a serious problem to the communities and the people in the area relies mostly on rivers, dams, dugouts, hand-dug wells and some boreholes. The dispersed nature of the settlement in these rural communities makes groundwater not only feasible but also generally available in dry season, relatively high quality and the most economic source of potable

water. Aside these however, agriculture which is the pivot of the local economy is still at an infant stage because of over reliance on rain-fed agriculture and basic farm implements.

2.2.2 GEOMORPHOLOGY AND CLIMATIC SETTING

The project area falls within the forest-dissected plateau. The area has undergone several years of erosion rendering the area to uniformly reduced heights. The topography of the area has elevation varying within 240 - 300 m above mean sea level. This geomorphological setup is characterized with forest vegetation, which has prevented sheet erosion rendering the area as a dissected plateau (Dickson and Benneh, 2004). Generally, most of the beneficiary communities are covered with lixisols soil type apart from Nnfodwo and Amangoase, which are covered with acrisols soil type.

The climate of the area is of wet-semi equatorial type (Dickson and Benneh, 2004). This climatic condition is characterized with a bi-modal rainfall pattern. The mean annual rainfall varies within 1250 – 2000 mm. The major rainy season is experienced from May to June with the minor rainy season experienced in September and October.

2.2.3 WATER ACCESSIBILITY

Essentially, borehole yields are often limited because flow of groundwater is largely limited to joints and cracks inside the crystalline rock formations. Groundwater supplies may be higher in the minor sedimentary deposits of the coastal basins (British Geological Survey, 2002). In the tropical southern part of the country, handpump tubewells and dug wells are in common usage, however surface water is still utilized in parts where tubewells are missing or not living up to expectations (British Geological Survey, 2002).

Assessing the water situation in the district, it was revealed that, there are 317 water points (boreholes/pipe-born) in the district and only 22% of the total population have access to this potable water while 78% fetch water from rivers, streams, wells and ponds (Figure 2.10). Out of the 22% of the total populations who have access to safe drinking water 21.5% depend on pipeborne water while the remaining 78.5% use borehole (Tain District Assembly, 2006).



Figure 2.10 Sources and nature of drinking water in the communities
The majority of these sources especially those focused around surface water assets are contaminated and are the sources of water-borne infections which is so common in the rural communities (Dapaah-Siakwan and Gyau-Boakye, 1999).



Figure 2.11 (a) People waiting to fetch water (b) people traveling distance to access water facility.

Information from the region shows that, 45% of the whole populace walks less than 50 m to access water from water facilities. Additionally 46% walk between 51 m – 1 km to access water and 7.6% travel between 1.1 km – 2 km to access water facility (Tain District Assembly, 2006). This means that more human hours which should be used in profitable ventures is, wasted to access water facility and fetching water (Figure 2.11). Effectively, this implies that, poverty will be high in the area. This suggests that there is the necessity to give more clean water to ease convenience for the people in the area.

2.2.4 GEOLOGICAL AND HYDROGEOLOGICAL BACKGROUND

2.2.4.1 Regional geology

Geology plays an essential role in the determination and occurrences of groundwater, and hence possible quantity and quality of groundwater. Ghana lies within the eastern domain of the Main Shield, which occupies the southernmost third of the West African Craton (Hirdes *et al.*, 1993). A

larger portion of the country comprises of Precambrian formations. In the middle of the country the downwarping of the basement (the Voltaian basin) is filled up by thick continental and marine sediments of the Middle Devonian (Erdelyi, 2010). The geology is dominated by ancient crystalline rocks, incorporating mostly metamorphosed sediments and granite. Minor occurrences of later unconsolidated sands, clays and gravels are limited to small zones along the coast (British Geological Survey, 2002).

These are the basement crystalline rocks associated with the West African Craton and covers 54% of the country and the Paleozoic consolidated sedimentary formation, which was formed in a depression of the West African Craton and covers about 45% of the country (Obuobie and Boubacar, 2010). The basement crystalline rocks are of Precambrian age and consist of granitogneiss-greenstone rocks, schist, phyllite, quartzite, strongly deformed metamorphic rocks and amorogetic intrusions (Obuobie and Boubacar, 2010; Key, 1992). The remaining 1 % is covered by minor provinces, such as the (a) Cenozoic, Mesozoic and Paleozoic sediments along the coast, and (b) Quaternary alluvium along major stream courses (Kankam-Yeboah *et al.*, 2003).

On the basis of the rocks genesis, characteristics and chemical compositions the major geological provinces are further divided into subprovinces. These are locally named as Birimian, Dahomeyan, Buem, Togo Series, Tarkwaian, Granites, Voltain, Coastal Block Fault, Coastal Plain and Quaternary Alluvium (Kankam-Yeboah *et al.*, 2003). Figure 2.12 shows a simplified geological map of Ghana.

2.2.4.2 Geological and hydrogeological formations of Tain district

The area falls under Birimian and Tarkwain rocks. The Birimian is the most mineralised formation in the country and comprises very thick isoclinal folds and metamorphic sediments. The area is

underlain by collapsed schists, greenstones, phyllites and graywackes. The intrusive granitoids of this formation are very important in groundwater resources as they contain secondary discontinuities like fractures, joints etc. and therefore form permeable groundwater reservoirs (Amoako, 2008). The Tarkwain is made of meta-sediment rocks i.e. conglomerate, sandstone, quartzite and shale. The Tarkwain is derived from the Birimian (metavolcanics) as a result of Eburnean tectono-thermal event; an orogenic activity. These rocks develop secondary and tertiary porosities and as a result accumulate substantial volume of water (Amoako, 2008). Tarkwain is characterized with sandstone and siltstone (GSD, 2009). The region is underlain by folded phyllites, schists, greenstones and graywackes and gives it better conditions for storage of groundwater, positive for borehole prospects after concluding geophysical investigations and comprehensive hydrogeological mapping (Erdelyi, 2010).

With the exception of Menji, Kwametenten and Kwadwokrom-Nkona, which are underlain by Tarkwain rocks, the rest of project communities in the district are underlain by rocks associated with the Birimian Formation. Hydrogeologically, the rocks underlying the study area forms part of the Complex basement, which underlies about 54 % of Ghana (Gill, 1969). The intrinsic porosity and permeability of these rocks had been enhanced by geo-tectonic event, which has facilitated groundwater development. The Birimian rocks are highly folded, generally foliated and fractured (Gill, 1969). An hydrogeological assessment conducted on the hydrogeologic province and sub-provinces in Ghana indicated that boreholes drilled in the Birimian sediments had yields varying between 0.41 – 29.8 m³/h with a mean yield of 17.3 m³/h. Similarly, aquifer systems associated with the Tarkwain formation had borehole yields varying within 0.45 – 23.6 m³/h with an average borehole yield of 7.4 m³/h (Dapaah-Siakwan and Gyau-Boakye, 2000). However, with improved geophysical techniques to delineate zones of high groundwater potential, there is the tendency to drill high-yielding boreholes within these geologic framework.

KNUST



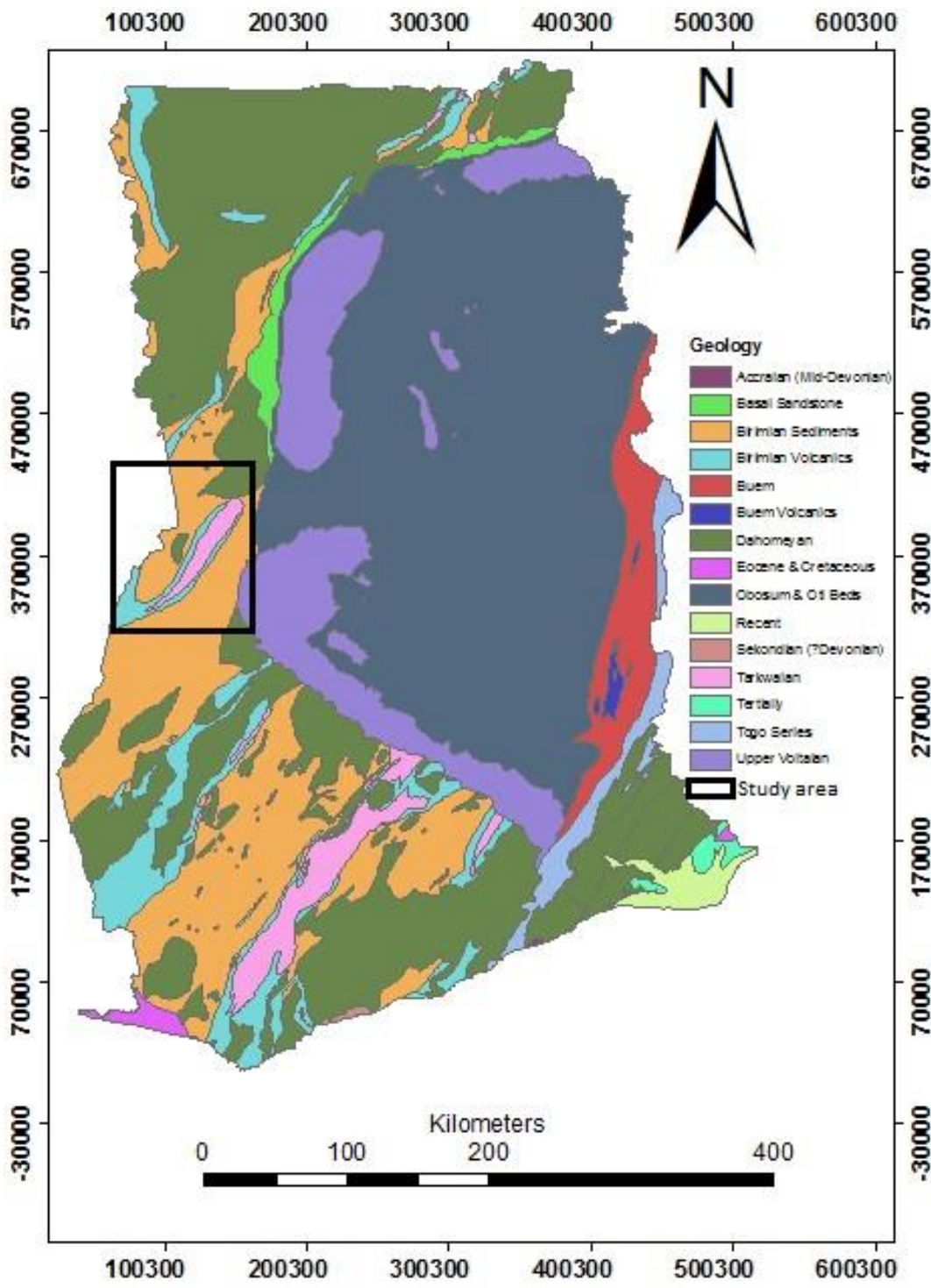


Figure 2.12 Geological map of Ghana (GSD, 2009)

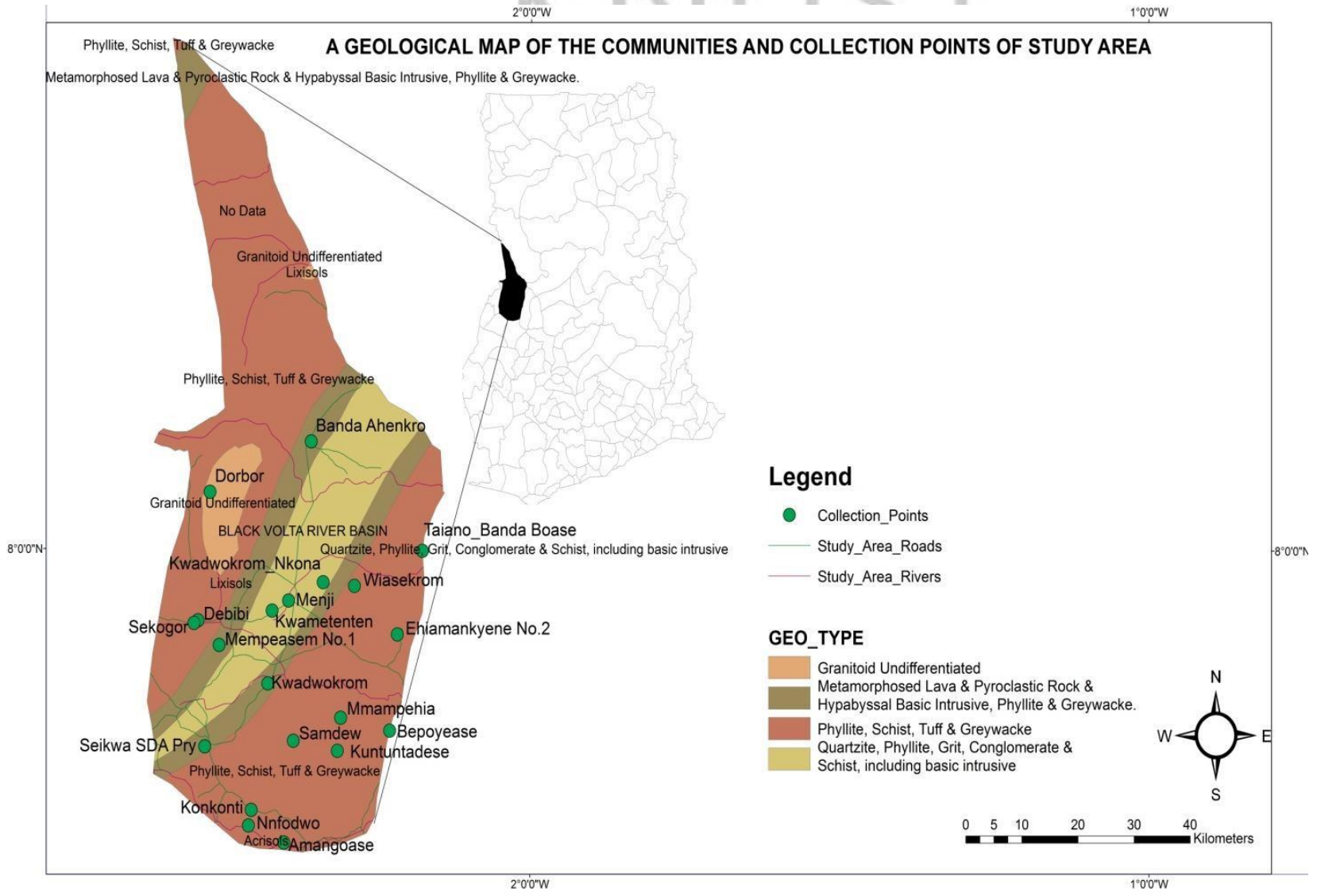


Figure 2.13 Geological map of the Tain district (GSD, 2009)

44 KNUST



CHAPTER THREE

3 METHODOLOGY

3.1 INTRODUCTION

The methodology consisted of desk study, field investigations (reconnaissance and geophysical surveys) and data processing. The field investigations covers a total of twenty (20) communities in the Tain District. The geophysical work was carried out in March, 2013.

3.2 DESK STUDY AND DATA COMPILATION

This study includes compilation and assessment of topographic and geological maps, existing borehole information and previous geophysical and hydrogeological work undertaken in the study area and finally the selection of the best electrode configuration for the geophysical investigated.

The motivation behind the study was to establish the current information about lineament patterns and fractures, the occurrence of suitable aquifers and their thickness, groundwater quality, the mean aquifer depth and the expected lithological sequences.

3.3 RECONNAISSANCE SURVEY

Visit was made to each of the study communities prior to carrying out the actual geophysical investigations which aided gathering information from the people about the groundwater situation. It comprised an assessment of topography, geology, hydrogeology, water points and soil surveys to discover sufficiently permeable zones that by virtue of their relative elevation or depression,

geological and hydrological history could be water-bearing. The main purpose of this exercise was to locate suitable target areas for geophysical investigations. The locations and directions of traverse lines were determined during the reconnaissance survey. In determining the directions of traverse lines, the GPS coordinate of the communities were recorded and located on geological map. This helped in understanding the lineament patterns and fractures.

Furthermore, social, logistical and accessibility considerations were also taken into account. This also included setting out traverse lines in the selected target areas and identification of pollution sources such as rubbish dumps, cemeteries, toilets etc. During the reconnaissance survey, Assemblymen and opinion leaders helped the field team to identify possible contaminant sources such as rubbish dump sites, cemeteries etc.

3.4 FIELD GEOPHYSICAL SURVEY

3.4.1 Introduction

The 2D Continuous Vertical Electrical Sounding (CVES) geophysical technique was employed to delineate suitable and most promising sites for the drilling of high-yielding boreholes to guarantee sustainable potable water to the beneficiary communities. The 2D CVES resistivity imaging survey seeks to carry out continuous vertical electrical sounding along a selected traverse and to produce 2D resistivity model sections of sub-surface geologic layers along the profile.

The LUND resistivity survey technique was used for the 2D sub-surface resistivity studies. This method uses a coupling of ABEM Terrameter SAS4000 resistivity meter and ABEM Electrode Selector ES 464 equipment and a maximum of 64 stainless steel electrodes, 12 V car battery, two

(2) sets of 100 m electrical cables and electrode jumpers (Figure 3.2). GPS was also used for locating profile line. This technique runs both profiling and vertical electrical sounding concurrently to produce a high resolution 2D resistivity model section of the surface. Several electrode arrays such as Wenner, dipole-dipole etc. are available to carry out this survey.

The ABEM LUND equipment consisting of two (2) electrical cables of length 100 m each was used for the field measurements depending on the depth of investigation. With the two cables used, only 41 electrodes are utilized and the depth of probe is about 29.0 m. However, if four cables are used then an approximate depth of 65.3 m would be investigated.

The cables have take-outs of 5 m intervals at which electrodes are connected to the ground using cable jumpers. With the aid of the electrode selector all the electrodes would be checked for poor contacts before measurements are taken.

3.4.2 The Field Procedure

A total number of twenty two (22) profile lines of CVES using 42 stainless steel electrodes, sets of cable jumpers, and two (2) electrical cables each of length 100 m were used. The Wenner configuration was used to carry out this investigation. During the measurement of the apparent resistivity, the two (2) electrical cable were laid along a designed profile and were then linked to the ground using the electrodes through sets of cable jumpers at 5 m repeated take-out (Figure 3.1).

The resistivity meter coupled with electrode selector and powered by 12 V car battery was used for the measurement of the apparent resistivity of the subsurface. Measurements were possible

after all the electrodes were connected via the take-outs and the terrameter and the Electrode selector are coupled together along a symmetrical spread.



Figure 3.1 Profile line with jumpers connecting cable take-outs to steel electrodes

Care was taken in the field to minimise the error in measurements by injecting appropriate current into the ground depending on the terrain. The contact between the electrode cables, electrode take-outs and cable jumpers were checked for dirt and oxide and cleaned when needed as they have effect on the data quality. The electrode test was performed to check the possibility of current flowing through all the electrodes. Poor ground contact was improved by changing the position of the poor contact electrodes sometimes connecting additional electrodes to the takeout to get sufficient contact.

The terrameter routinely changes the electrodes to function as current and potential pairs (Aning *et al.*, 2013). Measurements are automatically taken by the equipment and stored in the terrameter with the help of special electrode selection called protocols. This protocol makes series of electrode combinations between the currents and potential electrodes. Files in the terrameter are saved in binary formats with the file extension *.s4k*. This format is not compatible with the RES2DINV so it has to be converted to a convenient format.



Figure 3.2 Set up of The ABEM LUND resistivity imaging equipment

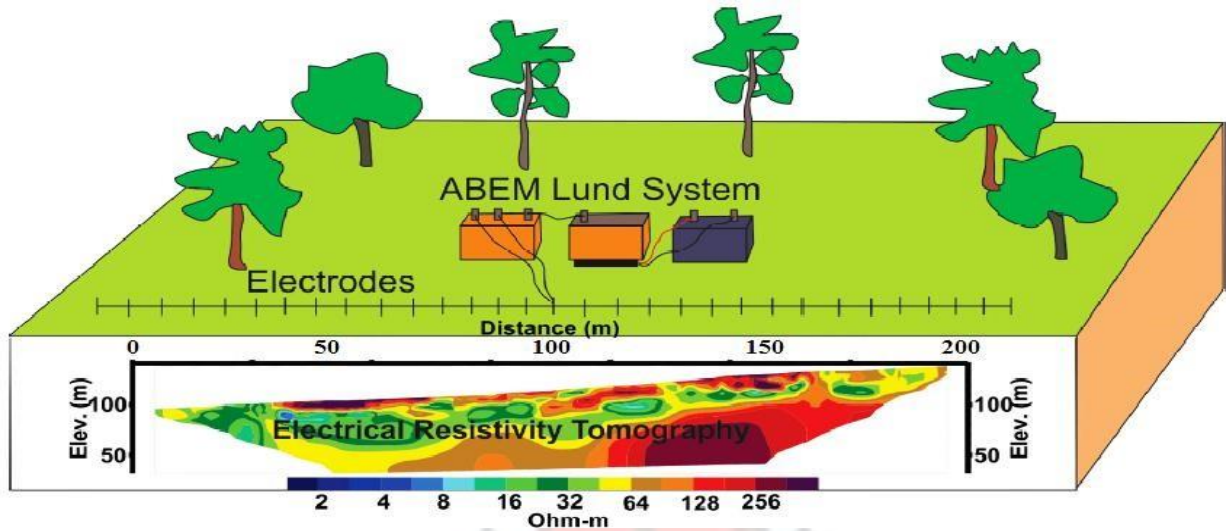


Figure 3.3 Sketch of multi electrode array showing the set-up and a possible electrical resistivity tomography (ERT) model obtained after inversion (Aning *et al.*, 2013).

3.4.3 Data processing

The recorded data for each profile from the LUND imaging survey was downloaded at site from the Terrameter using special SAS4000 Terrameter Utility software via a communication cable onto a personal computer (Laptop). The downloaded data was then converted from *.s4k format into RES2DINV format (*.DAT format), which is compatible with the inversion software.

Bad data points were effectively identified as they showed up as stand out points (Figure 3.4) in light of the fact that the apparent resistivity values were displayed in the form of profiles for every data level. *Exterminate bad datum points* feature in the RES2DINV was used to remove negative resistivity readings, extremely high and low resistivity readings from the data set before the resulting data were inverted. The elimination of the bad data points is necessary because it affects the data quality. Such erroneous resistivity values might be as a result of bad electrode ground

contact along the profile because of the dryness of the top layer, shorting across the electrical cables as a result of moisty ground situations and malfunctioning of some of the electrodes (Geotomo Software, 2010).

The geo-electrical resistivity inversion software was then used to carry out the inversion to produce 2D resistivity model-sections. The inversion routine used by the program is based on the smoothness constrained least square technique (Loke, 2000). The inversion program uses both finite-differences and finite-element forward modelling technique. A forward modelling subroutine is used to calculate the apparent resistivity values, and a non-linear least- squares methods based on a quasi-Newton optimization method techniques is used for the inversion routine (Geotomo Software, 2010).

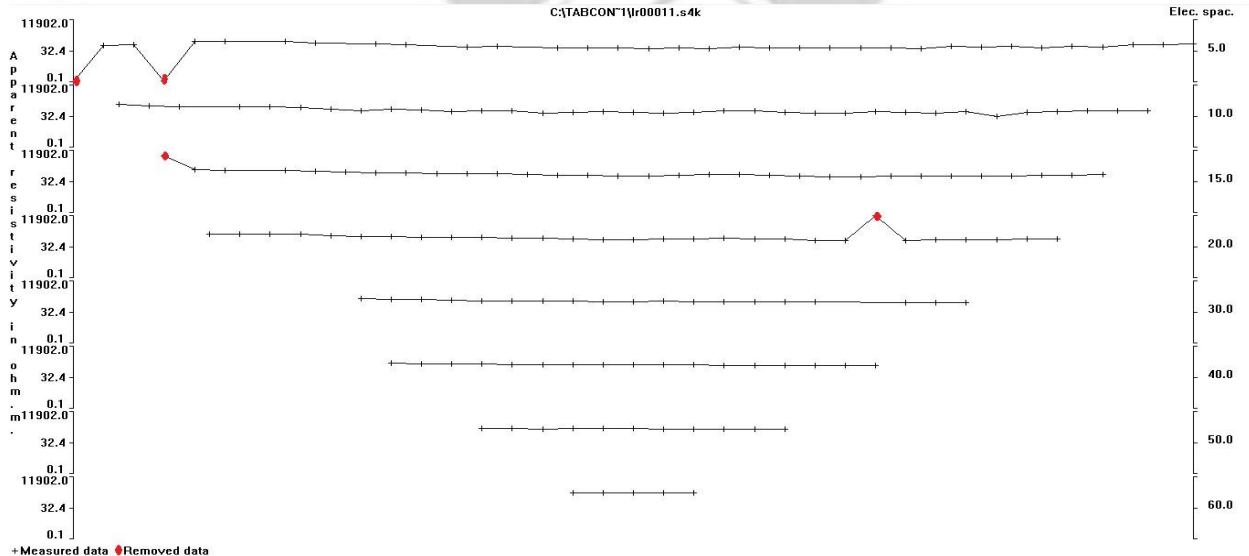


Figure 3.4 A sample of multiple electrode field data with some bad data points.

The computation of the sensitivity matrix for the entire iterations was done using the GaussNewton method. Model refinement was used to get optimum results as the option permits the selection of models with widths of half electrode spacing. Although the option increased the time of inversion

but was very significant due to the fact that it aided resolving changes in the close surface that might cause misrepresentations in the lower section of the model (Aning *et al.*, 2013).

Sharp variations in the resistivity values was reduced with help of the robust inversion constrain technique which lead to the production of model-sections with sharp boundaries among different zones with dissimilar resistivity values, but having virtually unvarying resistivity value within individual zones (Geotomo Software, 2010). This helped to produced models inversion with sharper and straighter boundaries. RES2DINV automatically creates a 2D model-section which provides true resistivity variation of the subsurface (Figure 3.3) (Ratnakumari *et al.*, 2012).

CHAPTER FOUR

4 RESULT AND DISCUSSION

4.1 INTRODUCTION

One fundamental tool in any groundwater development program is a good appreciation of geology. The geology determines the characteristics groundwater occurrence. Electrical resistivity is also a basic physical characteristic of rocks that can be directly correlated with rock lithological units and porosity, permeability, volume of water, level salinity and quantity of clay the key elements influencing the resistivity of these rocks.

Using the electrical resistivity equipment, 2D-CVES survey was carried out along selected traverses and the results were used to create 2D images of sub-surface geology along a profile with RES2DINV software. Apparent resistivity result gathered by the 2D dc-resistivity equipment were

processed to generate a model-section of subsurface resistivity that represents the true subsurface resistivity variation (Loke, 1997, El Mahmoudi *et al.*, 2011). The 2D resistivity tomography (model -sections) produced therefore has direct correlation to sub-surface geologic layers. The analysis and interpretation of the resistivity tomographies are therefore based on the knowledge of geology of the project area.

The 2D electrical resistivity technique is capable giving valuable information which is complementary to the in results acquired from using other geophysical technique in numerous geological conditions (Loke, 2010). The interpretation leads to the knowledge of the maximum depth at below at which it would be likely for groundwater to occur. This is because the resistivity of pure sand (not having shale and silt) and gravel saturated with fresh water ranges between 20 and several hundred ohm-meter. On the other hand, that impure sand (havng sale and silt) is much lesser (Sabet, 1975). Also the geoelectrical results allow us to verify the efficiency of the ERT in determining the boundaries between different geological layers (Sirhan *et al.*, 2011).

The profile lines (resistivity model-sections) figure (4.1 to 4.22) were named after the communities from which they were acquired. Directions and distances are measured from left to right along the profiles and depths are measured from the ground surface as shown in figure (4.1 to 4.22). For uniformity in the analysis and interpretation of resistivity pseudo-sections along the various profile lines, each profile data was processed separately however similar inversion procedures were employed in the processing of the entire model-sections. This helped to reduce differences and ambiguity to the minimum degree.

In the analysis and interpretation of the 2D resistivity model-sections, important consideration was given to the electrical resistivity values and not the colour representation because the same colour on each of the profiles in each of community represents different resistivity range of values.

Variation in the layers is represented by the varying resistivity values of the formations, which is associated with the various colours in the model-sections.

The modelled 2D resistivity sections were analysed to delineate resistivity and depths of various geological materials along the various profiles investigated. The sections were interpreted using the thicknesses of the various layers along the profiles coupled with the local geological conditions to select suitable sites with high groundwater potential.

4.2 ANALYSIS AND INTERPRETATION OF MODEL -SECTIONS

4.2.1 Menji profile A

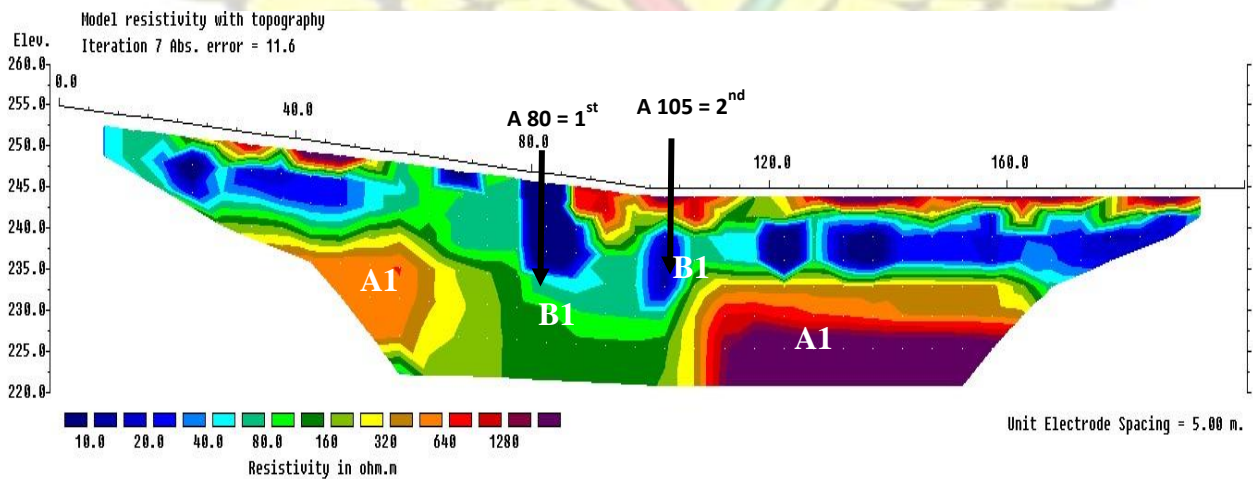


Figure 4.1 Resistivity model-section of Menji profile A

The model-section (Figure 4.1) depicts general varying low resistivity values $< 80 \Omega\text{m}$ from the surface up to a depth of about 15 m, beneath the profile. The thin high electrical resistivity $>$

600 Ωm observed at isolated places on the model-section in the near surface could be attributed to lateritic gravel materials at the surface as part were clearly seen on the surface during the fieldwork.

The high resistive structures on this section with resistivity values (600 -1300) Ωm labelled **A1**, at the base of the profile were interpreted as the basement rock. The low resistivity < 160 Ωm regions marked **B1** which extend beneath at around 80 and 105 m is bounded by the relative high resistive structures. The sharp resistivity contrast was therefore interpreted as a fracture; hence zone **B1** is good indication of possible geological structure, which could be a good aquifer for groundwater production. The points marked 1st and 2nd were selected for drilling in the order of preference.

4.2.2 Menji profile B

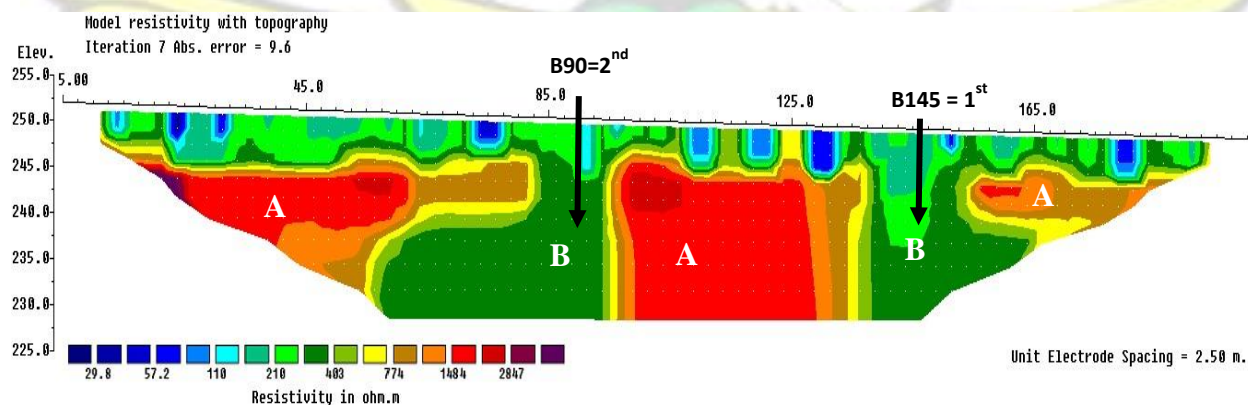


Figure 4.2 Resistivity model-section of Menji profile B

Model-section (Figure 4.2) shows varying low resistivity values < 400 Ωm from the surface up to a depth of about 7 m, beneath the profile. There are high resistivity zones on this section with values ranging between 800 and 3000 Ωm labelled **A**, which extends below the studied region. The low resistivity < 400 Ωm regions marked **B** extends to the base of the profile at around 90 and

150 m along the profile. These low resistivity anomalies are sandwiched between high resistivity zones and therefore could be a good aquifer for groundwater accumulation. The points B90 and B145 marked 1st and 2nd were selected for drilling in the order of preference.

4.2.3 Kwametenten profile A

The top surface of the model-section (Figure 4.3) shows moderate resistivity values ranging from about 80 to about 320 Ωm and to a depth of about 10 m indicating highly-weathered formation in the topmost layer section. The high resistivity zone of resistivity > 200 Ωm labelled **A** at the base of this model section is interpreted as semi-weathered bedrock. The low resistivity < 30 Ωm formation marked **B1** and **B2** flanked by relatively higher resistive zones could be interpreted as possible aquifer for groundwater production.

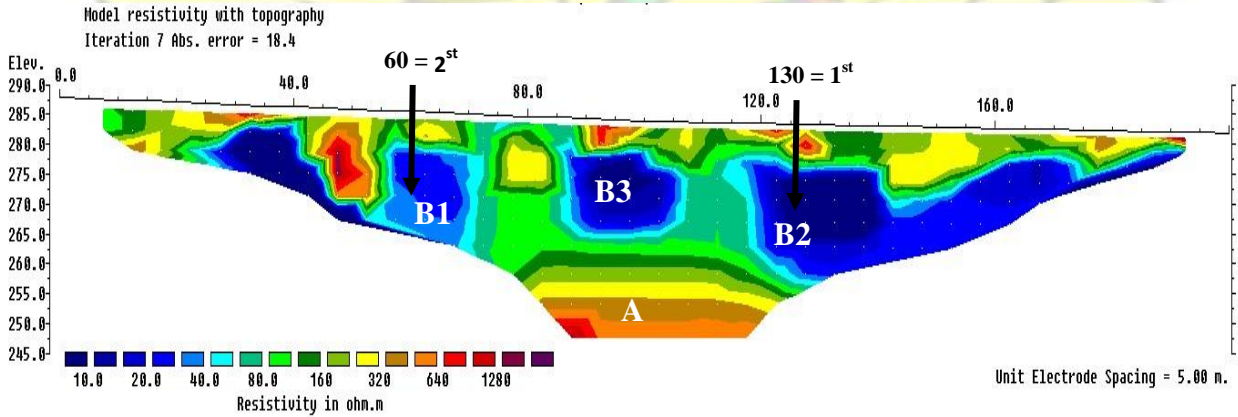


Figure 4.3 Resistivity model-section of Kwametenten profile A

B3 is also bounded below by relatively higher resistive semi-weathered bedrock and is much localized and therefore may not be a good potential source of groundwater as it is at a shallow

depth. Based on the lithology of the section, the points A130 and A60 marked 1st and 2nd were selected for drilling in the order of preference.



4.2.4 Kwametenten profile B

The resistivity model-section (Figure 4.4) reveals a general disorderly long range of resistivity 6 – 850 Ωm beneath the length the profile indicating high degree of weathering and fracturing of the subsurface formation. The high resistive structures on this section with resistivity values between 200 and 400 Ωm marked **C1**, in the near surface of the profile were interpreted as large masses of laterite as part were clearly seen on the surface. Also the very high resistivity (> 822 Ωm) geological formation observed between of 90 to 100 m on the profile line between depth of 5 m and 10 m labelled **C2** could be interpreted as a mass of hard compact rock.

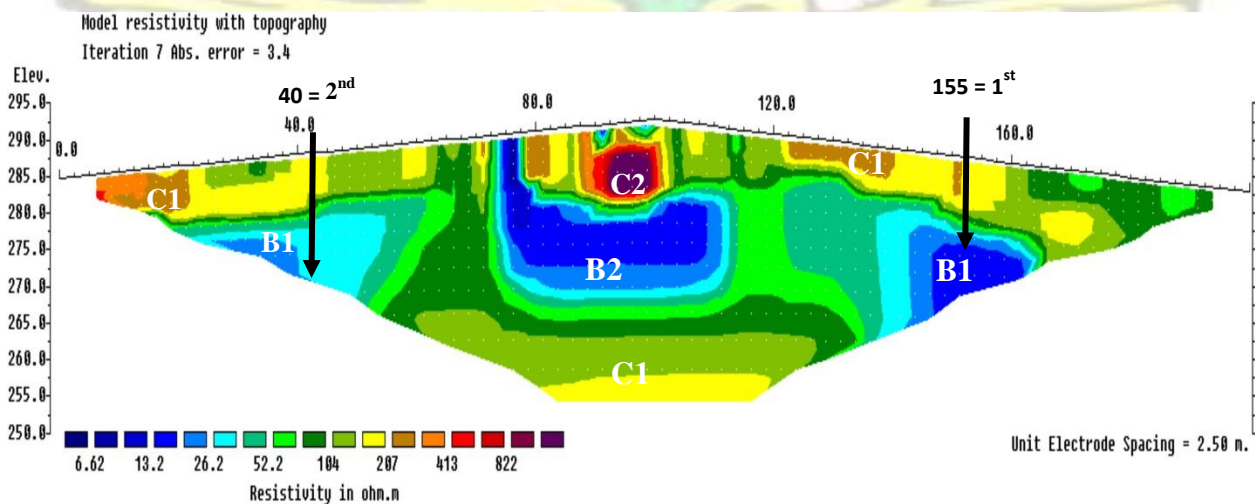


Figure 4.4 Resistivity model-section of Kwametenten profile B

The portions labelled **B1 and B2** are low resistivity (<30 Ωm) geological anomaly bounded with relatively high resistivity zones. These regions were interpreted as a weathered fracture and a good indication of water accumulation within these formations due to the lithological changes and

possible good aquifers for groundwater storage. The regions labelled **B1** may extend downward below the depth of investigation whereas **B2** is bounded above and below by relatively-higher resistivity zones. Based on the geological formation, the points B155 and B40 marked 1st and 2nd were selected for drilling in the order of preference.

4.2.5 Debibi (Health Centre) profile

The model-section (Figure 4.5) reveals varying low resistivity values < 40 Ωm from the surface up to a depth of about 8 m beneath the profile, which constitutes the saturated weathered top layer.

The resistivity model shows distinct degree of weathering and deformation of layers of rock which are clearly defined by their different resistivities between 75 and 160 m along the profile with the resistivity values fluctuating toward the end of the profile line. This weathered deformed material suggests a potential and promising site for groundwater as a result of its lithological nature.

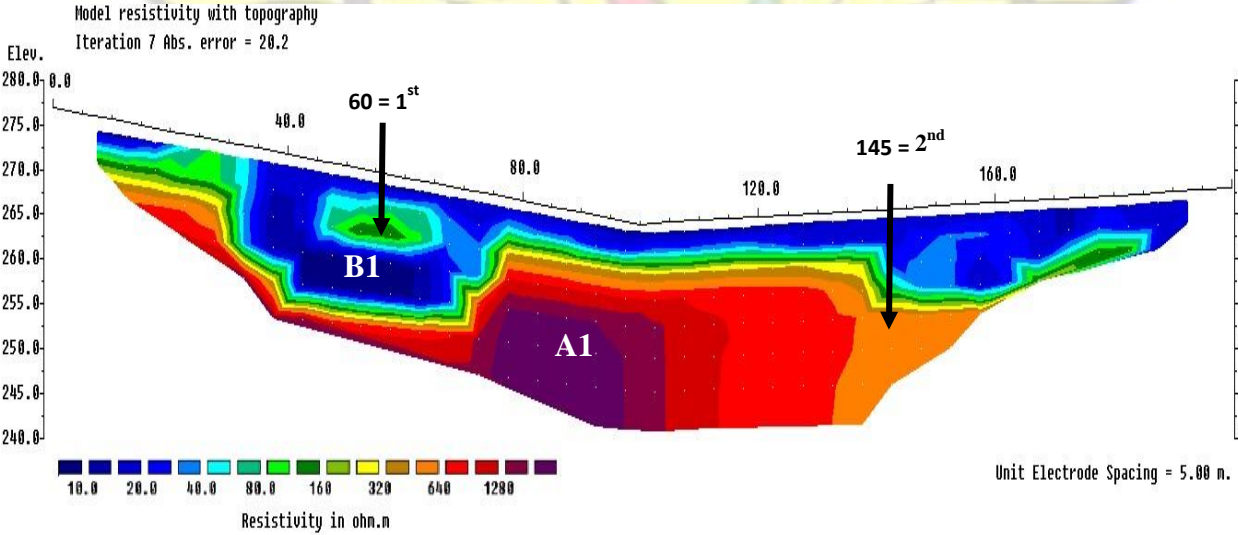


Figure 4.5 Resistivity model-section of Debibi (Heath centre) profile

The high resistivity zone of resistivity > 700 Ωm labelled **A1** at the base of this model section is interpreted as semi-weathered bedrock. The thick low resistivity layer with resistivity value <40

Ωm geological anomaly marked **B1** observed between 30 and 75 m beneath the profile and extends down to depth of about 25 m. This structure is engulfed by relatively higher resistive zones. This anomalous geological structure is located within the fractured basement rock formation and interpreted as possible good formation for aquifer (basement aquifers) and groundwater accumulation and was therefore selected for drilling. The points A40 and A145 marked 1st and 2nd were selected for drilling in that order of preference.

4.2.6 Sekogor profile

The top layer is highly-heterogeneous showing resistivity of about 5 to 178 Ωm throughout the profile up to a depth of about 2 m as clearly seen on the model-section (Figure 4.6) indicating weathering. The moderately-high resistivity materials only limited to the surface of the profile could be a case of lateritic gravel materials at the surface.

The top layer is underlain by comparatively low resistivity $< 30 \Omega\text{m}$ layer between the depths of 2 and 12 m beneath the profile, indicating highly-weathered saturated zone. This could be aquifer but may not be a good potential source for groundwater production. This could explain why the existing borehole drilled to a depth of 50 m along the profile line is not productive.

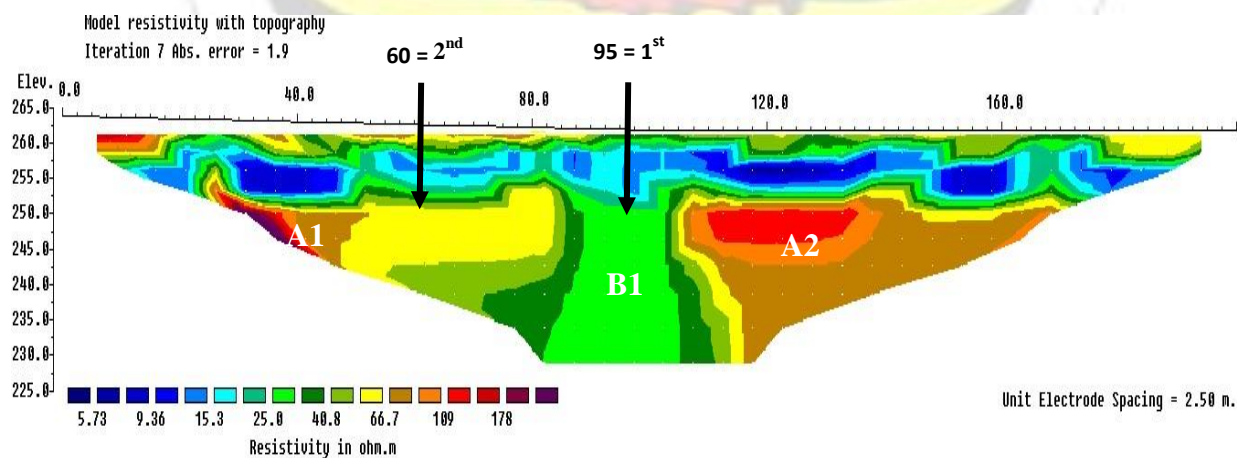


Figure 4.6 Resistivity model-section of Sekogor profile

There are high resistivity zones labelled **A1** and **A2** extending below the depth of resolution of the equipment on this section with varying resistivity values. The variation in the resistivity of region between portions marked **A1** and **B1** signifies varying degree of fracturing, which is a good indication of water flow within this formation due to the lithological changes and possible good aquifers for groundwater accumulation. The resistivity model-section shows a thick resistivity 25 – 45 Ωm structure marked **B1** between moderately high resistivity regions at about 90 and 105 m along the profile. This is interpreted as a fracture and could therefore be a good aquifer to target for siting borehole. Based on the geological formation, the points A95 and A60 marked 1st and 2nd were selected for drilling in the order of preference.

4.2.7 Ehiamankyene No. 2 profile

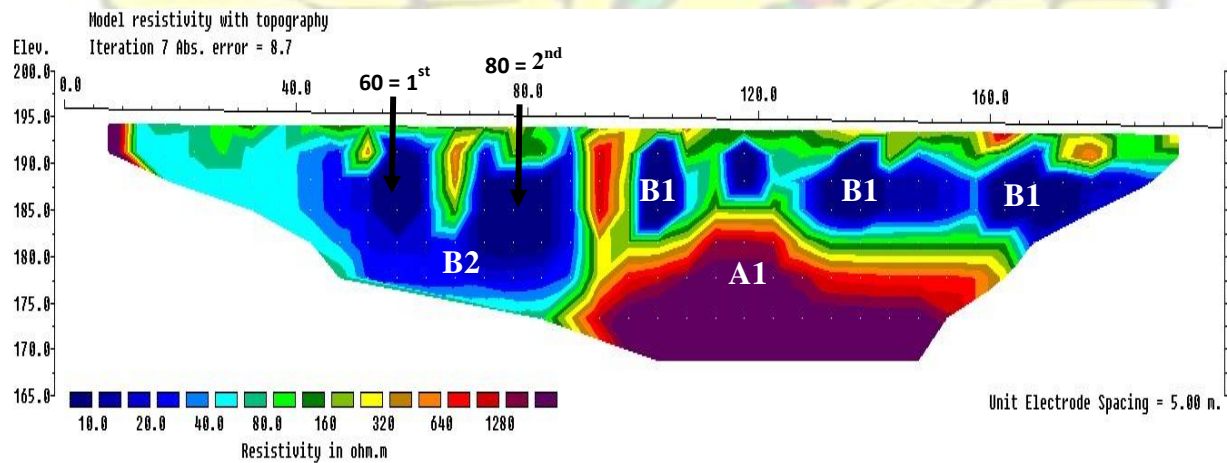


Figure 4.7 Resistivity model-section of Ehiamankyene No.2 profile

The resistivity model-section (Figure 4.7) displays a varying low resistivity top layer ranging from 10 to 160 Ωm to a depth of about 12 m from the surface indicating thick weathering of this top layer. There is a very high resistive body with varying resistivity values $> 1000 \Omega\text{m}$ tagged **A1**

observed between 85 and 160 m at a depth of about 20 m below the surface. This is interpreted as bedrock containing micro-fractures due to its low varying resistivity values.

Within the highly-fractured and weathered formation are patches of low resistivity of about 20 Ω m region denoted by **B1** between 100 and 140 m along the profile. These zones were interpreted as possible aquifer. These structures are bounded below by relatively higher resistive semi-weathered bedrock and are localized and therefore may not be good potential source of groundwater as they occur at shallow depths.

The resistivity model-section also brings to light a thick varying resistivity low values $> 40 \Omega$ m formation marked **B2** between 40 - 85 m, which extend below the depth of resolution of the equipment. The thick layer of very low resistivity formation is interpreted as possible good aquifer for groundwater accumulation due to the lithological fracturing within this formation.

The points A60 and A80 marked 1st and 2nd were selected for drilling in that order of preference.

4.2.8 Wiasekrom profile

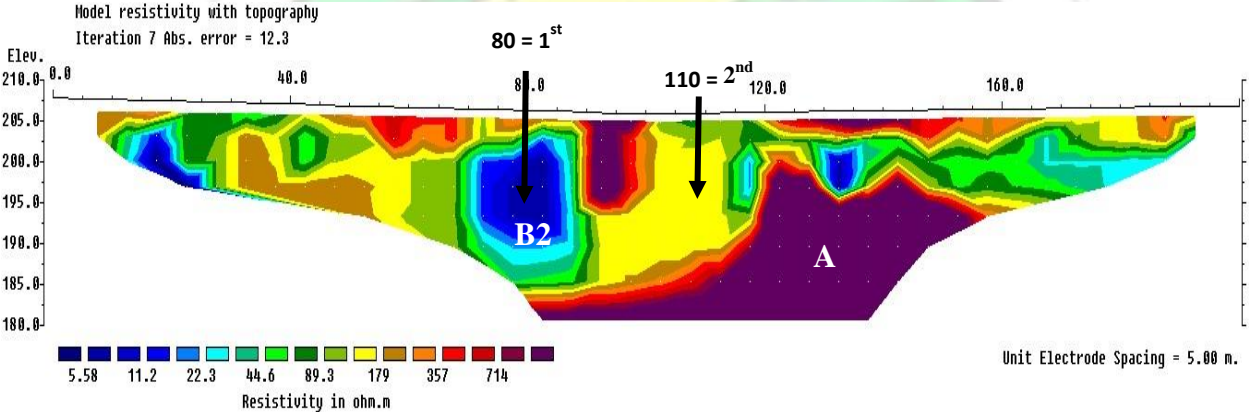


Figure 4.8 Resistivity model-section of Wiasekrom profile

The resistivity model-section (Figure 4.8) shows varying range of resistivity from 5 - 1000 Ωm , indicating very high degree of fracture and weathering of the subsurface. A dense low resistivity $< 44 \Omega\text{m}$ geological structural anomaly marked **B2** was intercepted between 70 m and 90 m along the profile line. The structure designated as **B2** engulfed by relatively-high resistivity zones is interpreted as possible good aquifer target for groundwater accumulation.

There is a protruded high resistivity $>1000 \Omega\text{m}$ geological feature at the base marked **A** observed between 75 and 155 m beneath the profile. This was interpreted as a basement rock based on the substantial resistivity contrast with the surrounding formation. This rock shows a significant differential fracturing associated with the host rock especially near the contact and such area may be hydrogeologically potential site for groundwater reserve and possible site for groundwater exploration. The points A50 and A110 marked 1st and 2nd were selected for drilling in the order of preference.

4.2.9 Mmaampehia profile

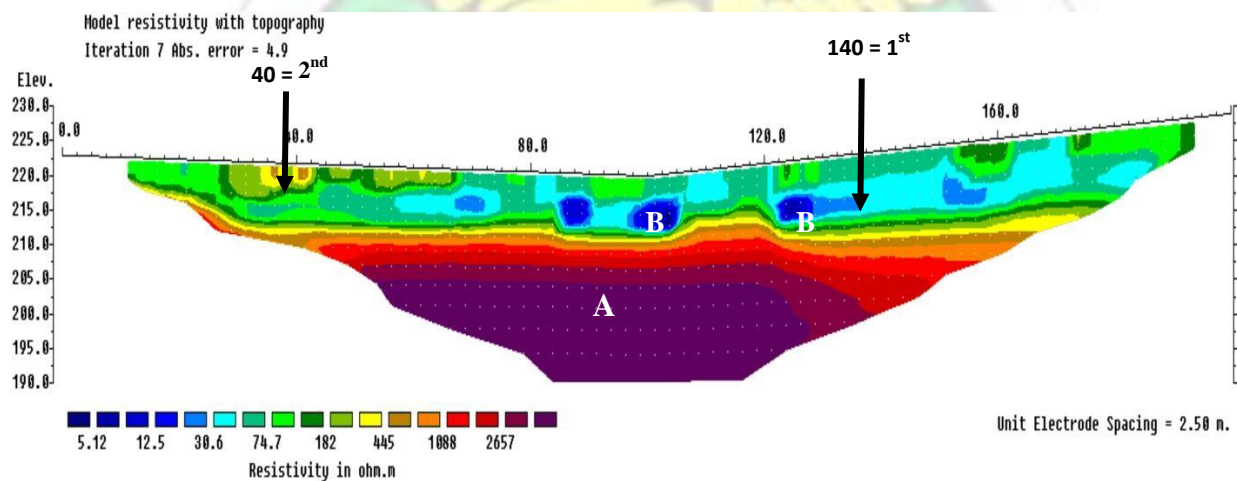


Figure 4.9 Resistivity model-section of Mmaampehia profile

The model-section (Figure 4.9) produces three different geological layered rock which are clearly defined by their different resistivity layers at the various depths. The model-section displays wide range of resistivity values from 5 to 450 Ωm to depth of about 10 m from the surface. This layer can be interpreted as highly heterogeneous soil formation derived from intense weathering of the underlying rock material. The model-section further reveals portions of low resistivity $< 30 \Omega\text{m}$ zones designated **B** found at isolated places within weathered top soil formation which can be interpreted as conductive isolated rock pockets.

The intermediate layer shows different subsurface materials with moderate resistivity with small changes in resistivity in the range 182 to 2000 Ωm at depth of about 15 to 25 m. This layer also appears broader between 30 - 60 m and 120 - 170 m along the profile line and was interpreted to have undergone some deformation as observed from the pattern and was interpreted as conceivable aquifers target for groundwater accumulation.

There is dense high resistivity $> 2657 \Omega\text{m}$ layer denoted by A at the base of this model-section. This high resistivity rock layer possibly representing the fresh rock material with no structural patterns gives no indication of fractures and joints which are indications for aquifers. despite the shallow overburden thickness, the points A140 and A80, marked as 1st and 2nd were selected drilling.

4.2.10 Bepoyease profile

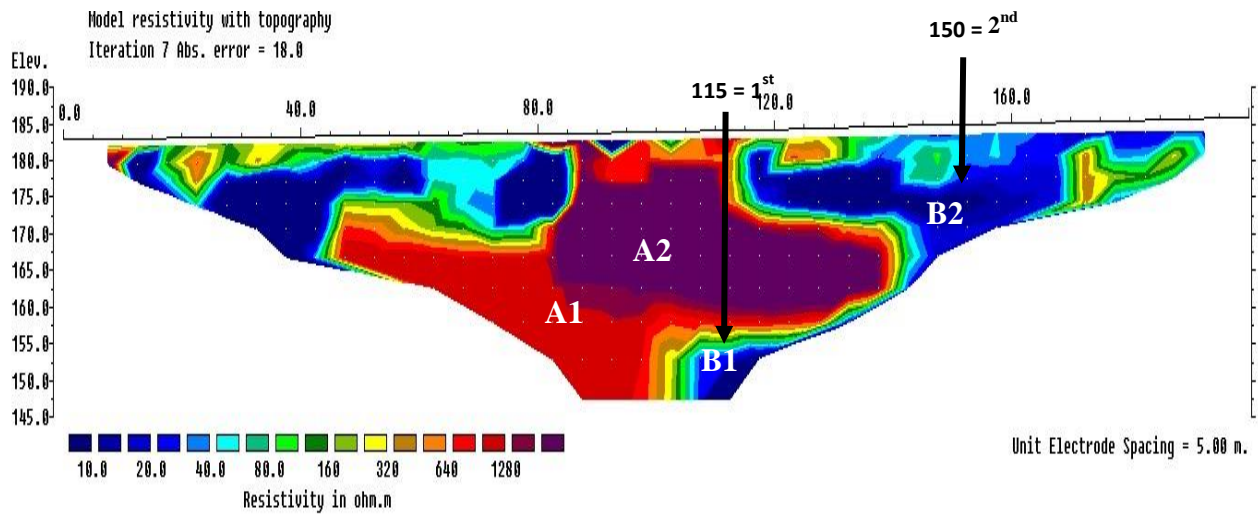


Figure 4.10 Resistivity model-section of Bepoyease profile

The model-section reflects high heterogeneities with large resistivity variation of the subsurface formation (Figure 4.10). The model-section depicts a high resistivity $> 600 \Omega\text{m}$ marked **A1** originating from deeper depth between 45 and 140 m along the traverse showing prominent 2D geological structural anomaly protruding towards both ends of the profile from the centre .

Underlain this massive body at a depth of about 35 m and between 105 – 115 m, is a low resistivity zone $< 40 \Omega\text{m}$ labelled **B1**. The sharp resistivity contrast acts as weathered saturated material suggesting a hydrogeologically potential site for groundwater reserve and target for groundwater exploration. This low resistivity zone is also seen to be connected to the surface through a highly-fractured zone between the 130 and 170 m, which separates the units of the massive high resistivity formation. This fracture zone appears to be the recharging site of the aquifer. The points A115 and A150 marked 1st and 2nd were selected for drilling in the order of preference.

4.2.11 Konkonti profile

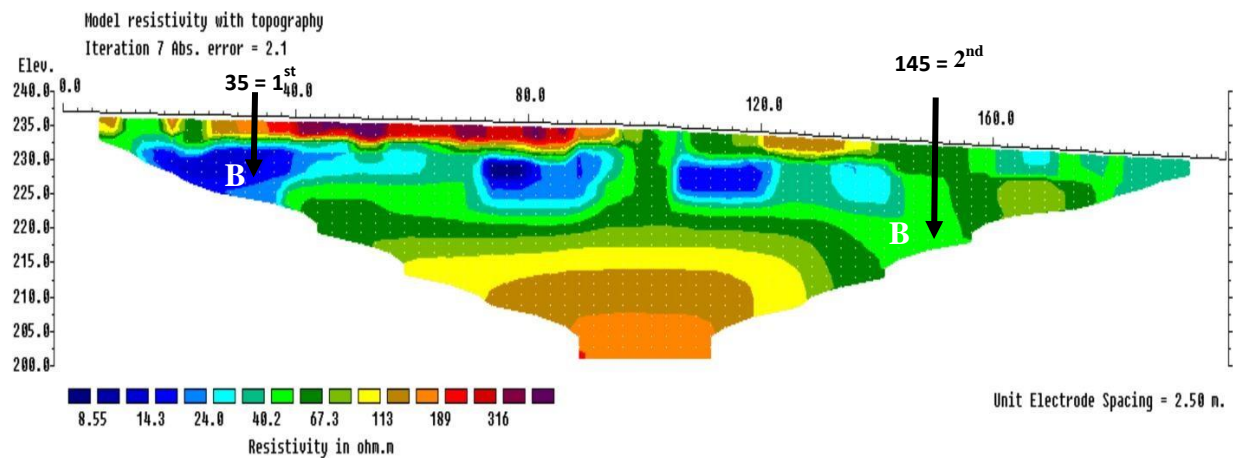


Figure 4.11 Resistivity model-section of Konkonti profile

The top surface is highly heterogeneous showing resistivity ranging from 8 to 320 Ωm to depth of about 15 m as clearly seen in (Figure 4.11) indicating highly-weathered top soil formation.

The relatively-high electrical resistivity values 189 to 316 Ωm observed in the near surface between 35 and 95 m could be lateritic gravel materials at the surface.

The model-section shows horizontal layers of different subsurface materials with small and sharp changes in resistivity at depth about 15 m to the base of the profile. These layers could be interpreted to be intercalations of different rock materials or showing the different weathered layers of rock at the subsurface.

There are regions with low resistivity $< 40 \Omega\text{m}$ tagged **B** below the resolution of the equipment between 15 and 35m and between 140 and 150m beneath the profile line. These regions reveal some degree of fracturing that could be interpreted as good material for an aquifer and was therefore selected for drilling. The points A35 and A145 marked 1st and 2nd were selected for drilling.

4.2.12 Nnfodwo profile

The relatively high lateral disparity in resistivity close to the surface to a depth of about 10 m as revealed in the model section (Figure 4.12) may reflect inhomogeneity and degree of weathering on this profile. There are high resistivity $> 500 \Omega\text{m}$ zones on this section denoted by **A1** and **A2** beneath the weathered top section. **A2** extends below the resolution of the equipment between 120 and 200 m along the profile line whereas **A1** is observed between the depth of about 10 and 20 m at around 50 and 90 m along the profile

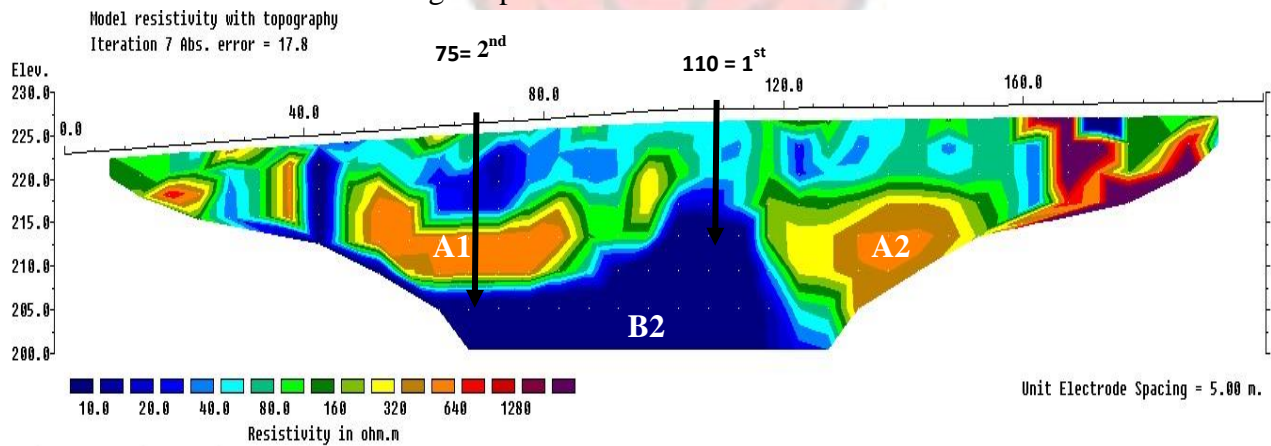


Figure 4.12 Resistivity model-section of Nnfodwo profile

. Underneath **A1** is a low resistivity $< 40 \Omega\text{m}$ regions marked **B** which stretched out below the study area at around 40 and 115 m along the profile. The geological structure is interpreted as possible water-bearing formation for groundwater accumulation and hence target for groundwater exploration. There is an indication of this formations connected to the surface through a fractured zone around 95 m. This fracture zone appears to be the recharging source of the aquifer. The points A110 and A75 marked 1st and 2nd were selected for drilling in the order of preference.

4.2.13 Amangoase (Kyekyewere) profile

The resistivity model-section (Figure 4.13) reveals varying high resistivity top layer ranging from (4 to 2000 Ωm to a depth of about 15 m indicating a high degree fractured and weathered top layer. This model-section exhibits a very high resistivity $> 800 \Omega\text{m}$ zone marked **A** in the left bottom the model-section, which is interpreted as bedrock. This high resistivity is also seen at the base of the profile at around 120 m.

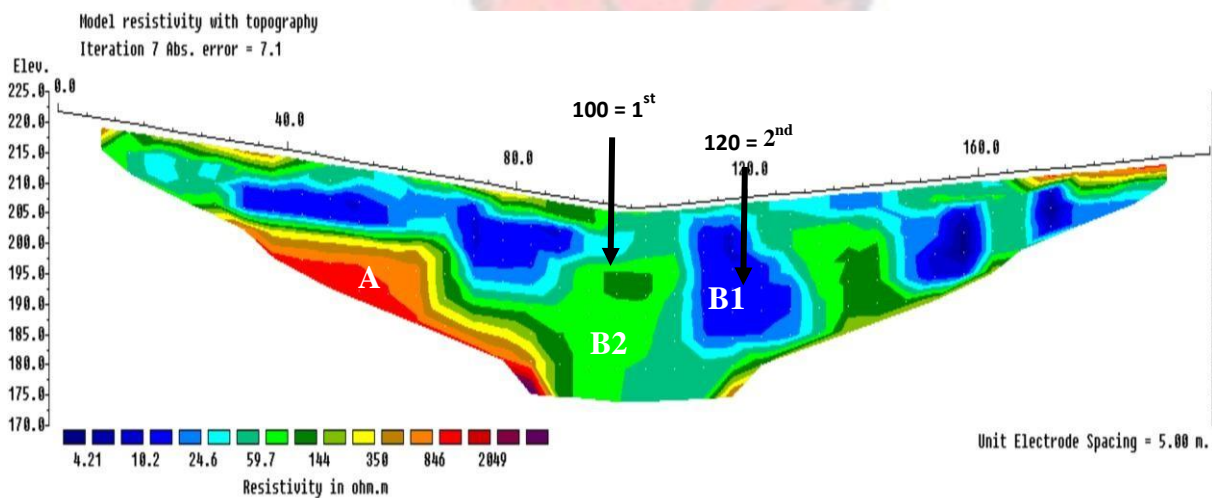


Figure 4.13 Resistivity model-section of Amangoase (Kyekyewere) profile

Thick but low resistivity geological structural anomaly ($< 25 \Omega\text{m}$) overlain by relatively high resistivity zones labelled **B1** is observed around 120 m along the profile line. This thick but low resistivity formation is interpreted as good aquifers for groundwater accumulation hence the region was selected for drilling. The resistivity model-section also shows a thick low resistivity of about $50 \Omega\text{m}$ geological structure between moderately high resistivity zones marked **B2** dipping downward at around 100 m along the profile line. The low resistivity zone could be fluid-filled or

clay deposit. However, this is interpreted as a fracture and a good indication of water flow within these formations due to the lithological changes and depressive nature and possible aquifers for groundwater accumulation. The points A100 and A120 marked 1st and 2nd were selected for drilling in the order of preference.

4.2.14 Seikwa profile

Generally, the resistivity model-section (Figure 4.14) depicts a varying high resistivity top layer ranging from about 400 to 2000 Ωm to a depth of about 5 m suggesting the presence of lateritic material in top layer.

Beneath this top layer is a thick layer of very low resistivity of about 9 - 20 Ωm. This layer is bounded above by weathered sediments topmost layer and below by distinct layers of moderate resistivities.

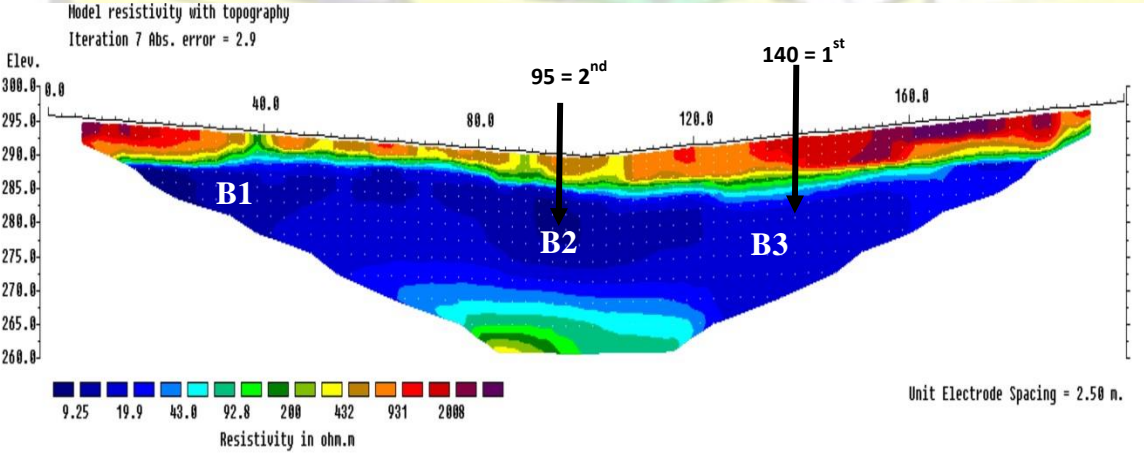


Figure 4.14 Resistivity model-section of Seikwa profile

Resistivity model-section shows zones of possible anomalies marked **B1**, **B2** and **B3** within the thick low resistivity zone. These spotted (anomalies) are bounded by relatively high resistivity region with quite lithological changes within formations and are interpreted as possible

groundwater bearing zone. The points A140 and A95 marked 1st and 2nd were selected for drilling in the order of preference.

4.2.15 Banda Ahenkro profile

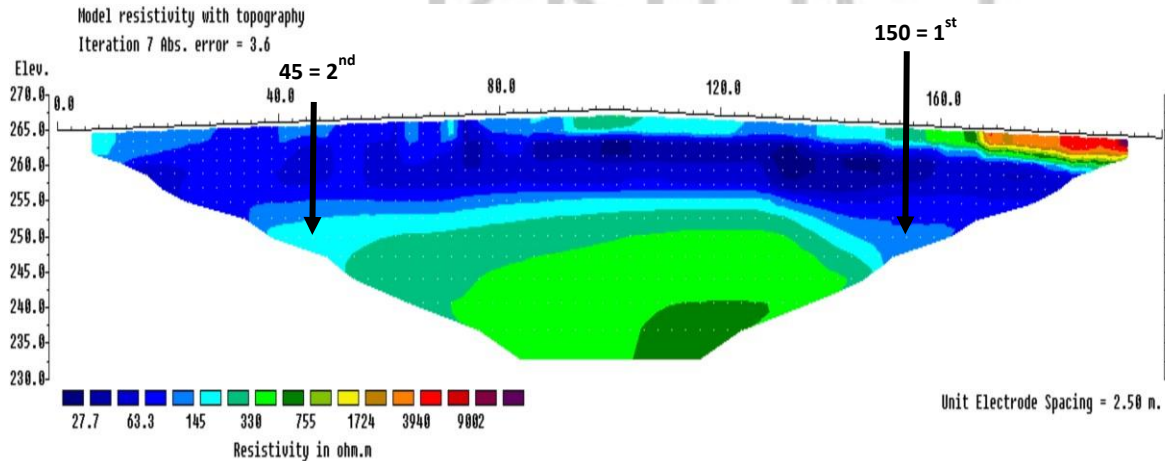


Figure 4.15 Resistivity model-section of Banda Ahenkro profile

The model-section (Figure 4.15) shows range of resistivity values from about 29 to 145 Ωm to a depth of about 15 m below the surface indicating weathered sediments, which could be derived from weathering of the underlying rock material. The resistivity model-section also shows a very high resistivity value of about 9000 Ωm to a few depth in the topmost right corners of the section, which is interpreted as hard rock material.

The intermediate layer beneath the weathered top sediments shows different subsurface materials with varying thicknesses along the profile line. The resistivity of these layers varies from moderately low resistivity of about 145 Ωm to high resistivity zones of about 755 Ωm between the depth of 15 and 40 m. Resistivity model-section (Figure 4.15) reveals that, the layers dip downward between 40 to 75 m and between 140 to 160 m along the profile line. These zones were therefore interpreted to be possible geological structure, which could be a target drilling.

The points A150 and A45 marked 1st and 2nd were selected for drilling in the order of preference.

4.2.16 Kwadwokrom-Nkona profile

The resistivity model-section (Figure 4.16) shows very low resistivity values of $< 60 \Omega\text{m}$ from the top to depth of about 10 to 15 m below the surface. This extremely low resistivity formation is separated by comparatively high resistivity $> 320 \Omega\text{m}$ weathered fractured zone between 75 and 110 m along the profile, which is interpreted to have emanated from deeper underlying hard rock.

There are two protruded high resistivity $> 500 \Omega\text{m}$ structures marked A between 40 and 105 m, which would probably be fractured bedrock based on the resistivity contrast with the surrounding formation. These probable fractures are hydrogeological potential sites for groundwater accumulation and targeted for groundwater exploration.

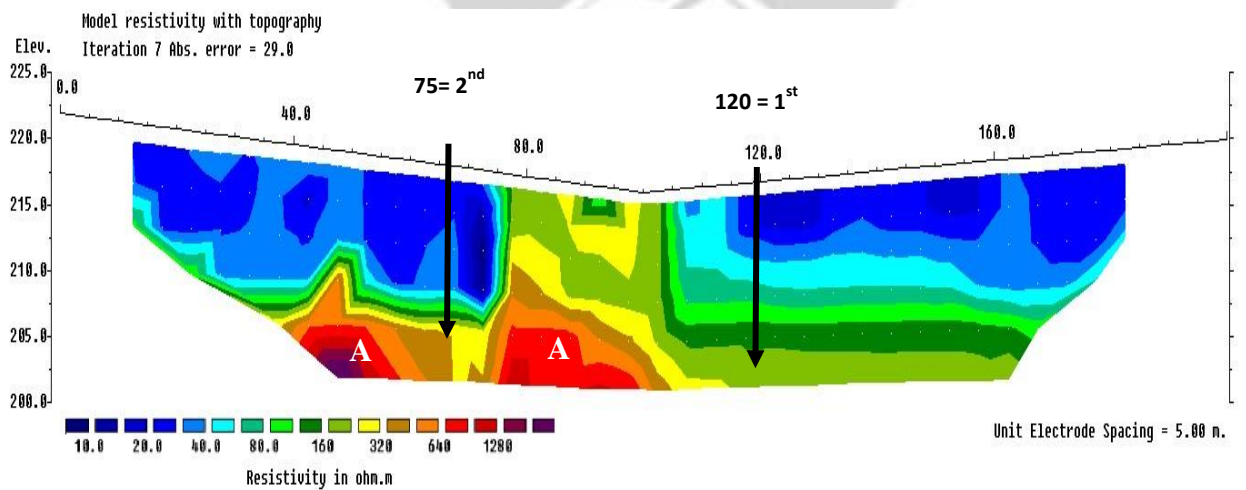


Figure 4.16 Resistivity model-section of Kwadwokrom-Nkona profile

The model-section also reveal horizontal layers of different subsurface layers with sharp changes in resistivity at depth of about 15 m to the base in the last half of the profile. These layers could be interpreted to be intercalations of different rock materials with varying resistivity values. This resistivity range could be interpreted to be good material due to lithological changes within these

formations. The points A120 and A75 marked 1st and 2nd were selected for drilling in the order of preference.



4.2.17 Mempeasem profile

The model-section (Figure 4.17) generally displays wide range of resistivity values from 1 to about 42 Ωm to a depth of about 10 m below the surface beneath the profile, which signifies high heterogeneous weathered top soil formation. Patches of very low resistivity values < 6 Ωm marked **B** observed at isolated locations within the weathered top layer could be moist clayey soil and may not be good aquifers for groundwater accumulation. The intermediate layer shows varying thin subsurface materials with moderate resistivity. However, there are small changes in resistivity in the range 12 - 192 Ωm at depth of about 15 m between 40 and 160 m, these may be an indication of intense weathering derived from the underlying rock material.

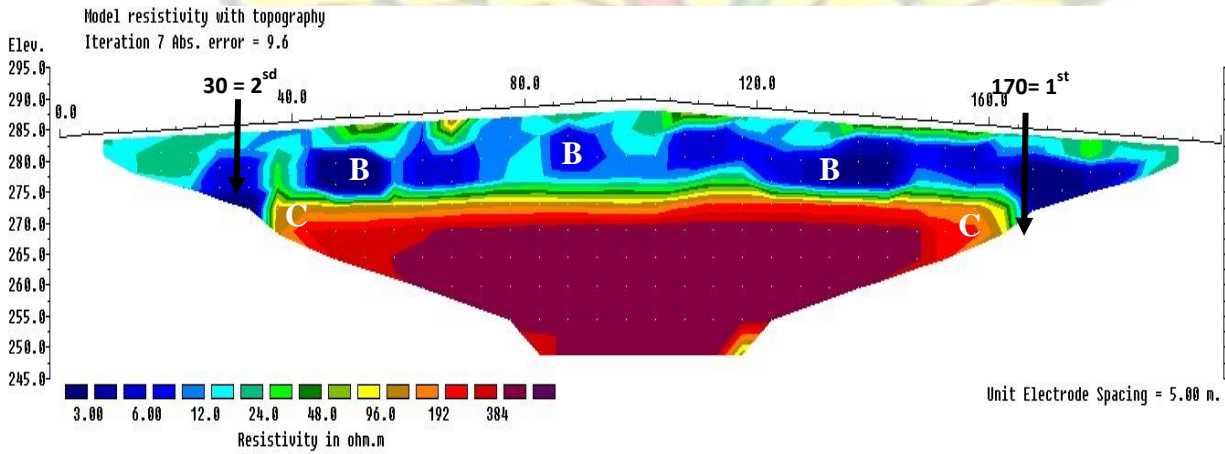


Figure 4.17 Resistivity model-section of Mempeasem profile

The resistivity model-section reveals differential vertical deformation and weathering associated with the host rock especially near the contacts around 40 and 160 m. Such areas are

hydrogeologically potential sites for good aquifers for groundwater accumulation for groundwater exploration. These regions are denoted **C** on the model-section. The points A170 and 30 marked 1st and 2nd are the selected potential aquifer site for drilling in the order of preference.

4.2.18 Kuntuntadease profile

The model-section (Figure 4.18) shows varying high resistivity geological layer with resistivity values with resistivity values higher than 400 Ωm from the surface up to a depth of about 15 m beneath the profile. This could be attributed to weathering effect and lateritic gravel materials in the top layer. There is a protruded high resistivity (> 400 Ωm) geological formation at the base designated **A** observed between 80 and 120 m beneath the profile. This was interpreted as fractured bedrock based on the geometry and the resistivity contrast with the surrounding formation.

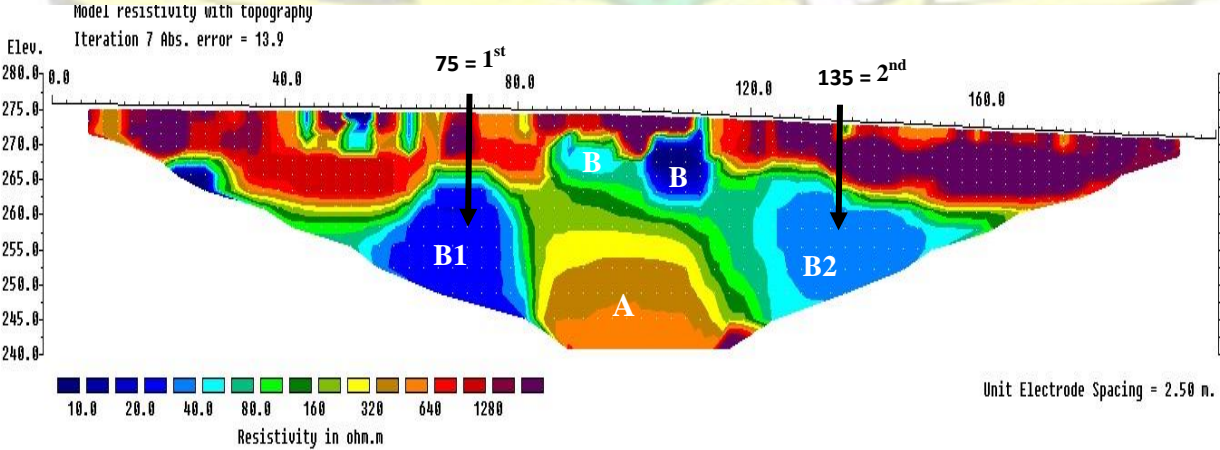


Figure 4.18 Resistivity model-section of Kuntuntadease profile
 The model-section further reveals portions of very low resistivity (< 40 Ωm) zones designated **B** found at isolated places which could be interpreted as moist clayey material and hence not targeted for groundwater exploitation. The resistivity model-section shows zones of possible anomalies marked **B1** and **B2** of resistivity of about 40 Ωm. These spotted anomalies, bounded by relatively

high resistivity are interpreted as potential sites for groundwater reserve and possible sites for groundwater exploitation. The points A75 and A135 marked 1st and 2nd were selected for drilling in order of preference.



4.2.19 Taiano-Banda Boase profile

There are high resistivity >1000 Ωm geological formation (Figure 4.19) from the base marked **A** observed between 40 and 100 m and around 160 m beneath the profile, which were interpreted as a possible fractured bedrock based on the resistivity contrast.

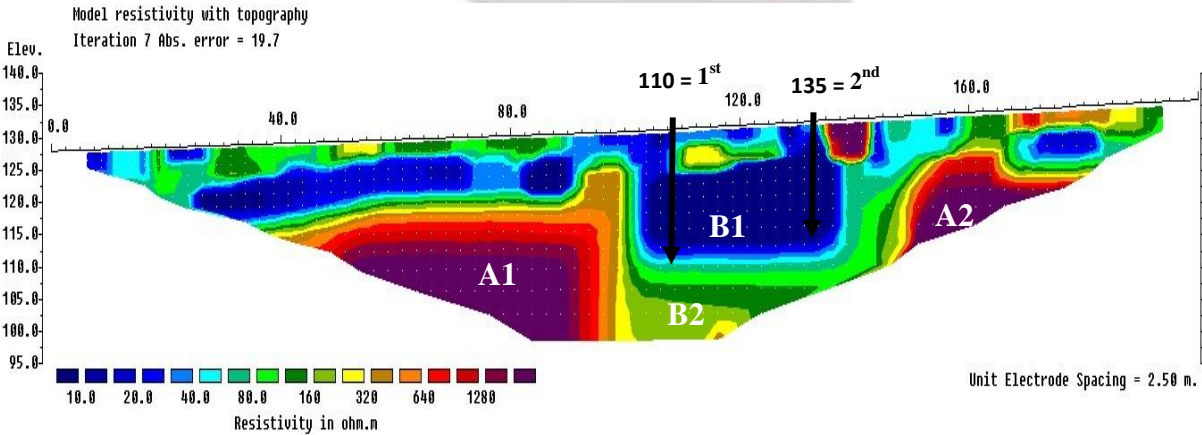


Figure 4.19 Resistivity model-section of Taiano-Banda Boase profile

The low resistivity (< 40 Ωm) regions marked **B1** observed between 90 and 130 m beneath the profile. This anomaly is sandwiched between high resistivity zones and therefore could be a good aquifer for groundwater exploitation. The fact that **B2** indicate considerable fracturing associated with the host rock near the contacts further suggest that zones **B1** and **B2** are potential sites for groundwater exploration. The points A110 and A135 marked 1st and 2nd are selected for drilling in the order of preference.

4.2.20 Samdew profile

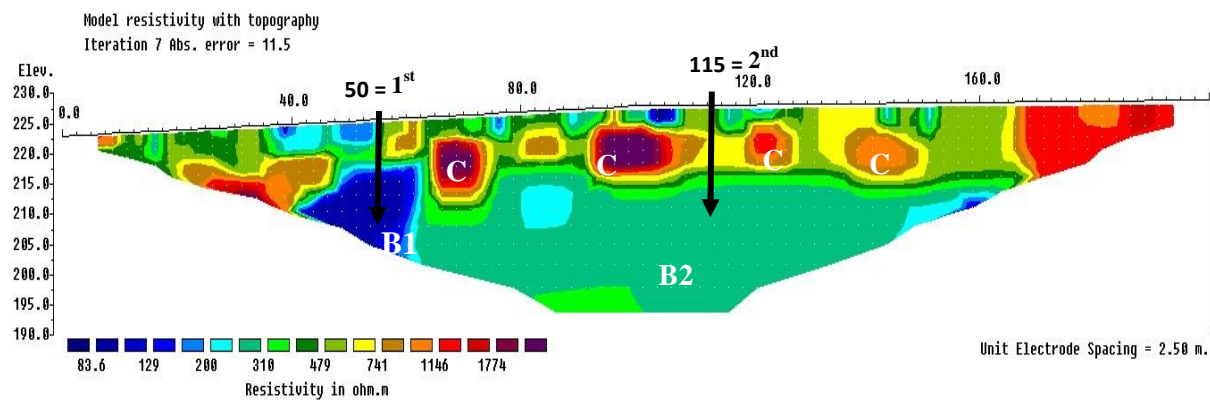


Figure 4.20 Resistivity model-section of Samdew profile

The model-section (Figure 4.20) portrays high heterogeneities with large resistivity variation from the surface up to a depth of about 20 m, beneath the profile reflecting a very high degree of fracture and weathering of the subsurface. The very high resistivity ($> 1000 \Omega\text{m}$) geological formation observed at isolated region labelled **C** could be interpreted as a pockets of hard compact rock materials.

The section marked **B1** observed beneath the thick fractured and weathered top layer between 60 – 80 m beneath the profile was interpreted as an aquifer for groundwater storage. This may be due to the fact that it can have the tendency of accumulating water from the weathered zone above.

The portion tagged **B2** is low resistivity ($< 200 \Omega\text{m}$) geological formation extending below the resolution of the equipment. This region reveal high degree of structural deformation and could be interpreted to be good aquifer, and it was therefore selected for drilling. The points A50 A115 marked 1st and 2nd are selected for drilling in the order of preference.

4.2.21 Kwadwokrom/Sulage profile

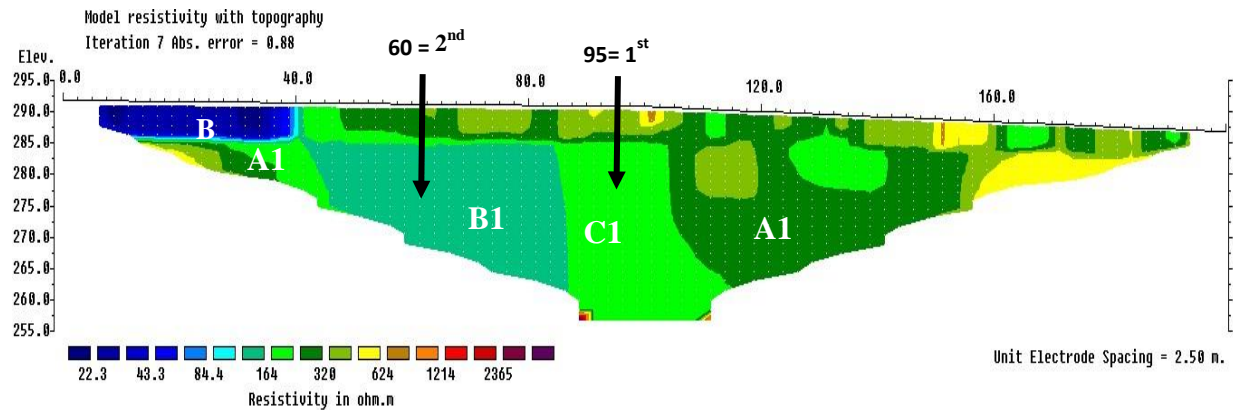


Figure 4.21 Resistivity model-section of Kwadwokrom/Sulage profile

The top surface is highly heterogeneous displaying resistivity ranging from 160 to 600 Ω m to depth of about 10 m from 40 m to the end of the profile (Figure 4.21). This indicates high weathered region derived from intense fracturing of the underlying rock material. The resistivity model-section also shows a very low resistivity value ($< 40 \Omega$ m) to a few depth in the topmost left corner of the section, which is interpreted as moist clayed material.

The resistivity model-section further unfold a number of vertical deformation structures designated **A1**, **B1** and **C1**. The region **C1** was interpreted as weathered deformed material and a good indication of water flow within this formation due to the lithological changes and serves as possible target for groundwater exploration. The zone labelled **B1**, which is probably more weathered than **C1** suggest that it will be potential site for groundwater accumulation. The points A95 and A60 marked 1st and 2nd were selected for drilling in the order of preference.

4.2.22 Dorbor profile

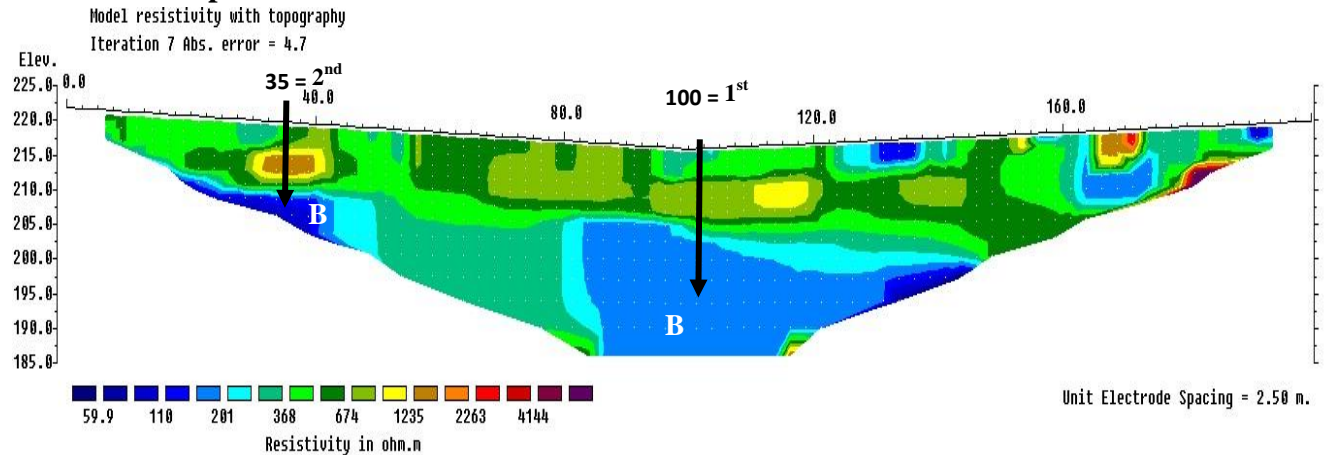


Figure 4.22 Resistivity model-section of Dorbor profile

The top surface is highly heterogeneous displaying resistivity values ranging from 300 to 3000 Ωm to depth of about 20 m beneath the profile as seen in (Figure 4.22), indicating highly weathered and fractured top layer.

The resistivity model-section also shows a thick low resistivity zone of about 50 Ωm resistivity marked **B** extending below the resolution of the equipment between 0 - 40 m and 80 - 150 m beneath the profile. The low resistivity zone appears to have undergone some deformation as observed from the pattern. Thus it was interpreted as a fracture and may be a good indication of water flow within the formation and possible aquifers for groundwater accumulation. The points A100 and A35 marked 1st and 2nd were selected for drilling in the order of preference.

CHAPTER FIVE

5 CONCLUSION AND RECOMMENDATIONS

5.1 CONCLUSION

The 2D resistivity technique produced substantial 2D model-section with high quality in terms of structural resolution. This lead to the demarcation of the layering of various lithological units; weathering layers, depth to bedrock and identification of important structures such as fractures and faults. These structures are quite substantial in groundwater exploration.

The 2D resistivity model sections of the various profiles in the study communities revealed that the geology of the area is underlain by highly-weathered, fractured, and local faulted zones. The study has established that the rocks forming the aquifer in the Tain District in the Black Volta Basin are mainly comprises weathering of the overburden and fracturing of the underlying bedrock. It therefore suggests that the hydrogeology of the project region is highly complex since the development of groundwater is generally due to secondary porosities.

The variation in thicknesses and electrical resistivities of the various geological formation (anomaly) of the sub-surface is attributed to structural deformation and weathering activities. This is evidenced by the highly-heterogeneous nature of the subsurface rock materials, high weathering of the overburden and fracturing of the underlying bedrock which does not only result from the metamorphosed nature of the Birimian and Tarkwaian rock formation but also for the fact that the study area falls within geological contact zone between Birimian and Tarkwaian formations. Such areas always characterised by high degree of frequent minor and major fractures.

The thicknesses and resistivity values of the aquiferous zones relative to the background resistivities suggest that, these geological structures could be targets for groundwater occurrence. In selection of the drilling points, much attention was placed on water-bearing structures located at deeper

depth on the basis that basement formation plays a major role in striking sustainable and quality yield groundwater.

2D-CVES imaging technique proved to be successful, resourceful, cost-effective and fast in groundwater exploration in delineating aquifers and mapping shallow subsurface resistivity anomalies in all the project communities. With the use of this improved geophysical technique to select the drilling points, it is expected that each of the beneficiary communities will be lucky to have a successful borehole.

5.2 RECOMMENDATIONS

The rms errors of some of the resistivity model were high. These were as a result of difficulty in transmitting the current in to the ground because of the dryness of the subsurface. It is necessary to conduct such surveys not in the dry period of the year and not also in the rainy season.

Induced polarization technique should be carried out alongside the resistivity measurement in order to ascertain whether the low resistivity zones are as a result of water or clay as this will minimize drilling dry wells.

Water from each successful well should be sampled for physico-chemical and bacteriological analyses to determine their safety and suitability for domestic and other uses.

REFERENCES

Alile, M. O., Jegede, I. S. and Ehigiator, O., 2008. Underground Water Exploration Using

- Electrical Resistivity Method in Edo State, Nigeria. *Asian Journal of Earth Sciences*.
- Amarachi, R. A. and Ako, B. D., 2012. Groundwater Investigation Using Combined Geophysical Methods. *Search and Discovery*, Issue Article #40914.
- Amoako, J. A., 2008. *Mapping Groundwater Quality in Northern Region of Ghana Using GIS*. MSc. Thesis (Kwame Nkrumah University of Science and Technology)
- Aning, A. A., Tucholka, P. and Danuor, S. K., 2013. 2D Electrical Resistivity Tomography (ERT) Survey using the Multi-Electrode Gradient Array at the Bosumtwi Impact Crater, Ghana. *Journal of Environment and Earth Science*, Volume 3.
- Anornul, G. K., Kabo-bah, A. T. and Anim-Gyampo, M., 2012. Evaluation of Groundwater Vulnerability in the Densu River Basin of Ghana. *American Journal of Human Ecology*, Volume 1, No. 3.
- Asomaning, G., 1992. Groundwater resources of the Birim basin in Ghana. *Journal of African Earth Sciences*, Volume 15, pp. 375-384.
- Baker Hughes INTEQ, 1999. *Geological Procedures Workbook*. Houston, TX 77073: Baker Hughes INTEQ.
- Bayewu, O. O., Oloruntola, M. O., Mosuro, G. O. and Watabuni, F. G., 2012. Groundwater exploration in Ago-Iwoye Area of Southwestern Nigeria, using Very Low Frequency Electromagnetic (VLF-EM) and Electrical Resistivity. *Int. Journal of Applied Sciences and Engineering Research*, 2012 www.ijaser.com, 1(3).
- British Geological Survey, 2002. Groundwater Quality: Ghana. *NERC 2000*.
- Bowen, D. G. (2008, Dec). Core Laboratories - Formation Evaluation and Petrophysics. Jakarta, Indonesia: Tarek. Retrieved from <http://www.scribd.com/doc/8592400/Core-Laboratories-Formation-Evaluation-and-Petrophysics#scribd> [Accessed 2013].

Cardimona, S., 2008. Electrical Resistivity Techniques for Subsurface Investigation. *Department of Geology and Geophysics, University of Missouri-Rolla, Rolla, MO.*

Dapaah-Siakwan, S. and Gyau-Boakye, P., 2000. Hydrogeological framework and borehole yields in Ghana. *Hydrogeological Journal*, pp. 400-416..

Dapaah-Siakwan, S. and Gyau-Boakye, P., 1999. Groundwater; solution to Ghana rural water supply industry? *The Ghana Engineer.*

Dewashish, K., 2012. Efficacy of Electrical Resistivity Tomography Technique in Mapping Shallow Subsurface Anomaly. *Journal Geological Society Of India*, September. Volume Vol.80, pp.304-307.

Dickson, B. and Benneh, G., 2004. *A New Geography of Ghana*. Edingburg Gate: Harlow, Essex CM20 2JE, England: Pearson Education Limited..

Djebbar, T. and Erle, C. D., 2004. *Petrophysics : Theory and practice of measuring reservoir rock and fluid transport properties*. second ed. Burlington(MA 01803): Gulf professional publishing/ usevier.

Dobrin, M. B. and Savit, C. H., 1988. *Introduction to Geophysical Prospecting*. Singapore: McGraw-Hill International Edition.

Driscoll, F., 1986. *Groundwater and Wells*. Minnesota: Johnson Division, St Paul.

El Mahmoudi, A. S., Al-Barrak, K. M. and Massoud, A., 2011. 2-D Electrical Tomography for Mapping of Aquifers at the New Campus of King Faisal University, Al Hassa, KSA. *International Journal of Water Resources and Arid Environments.*

Erdelyi, Research Institute for Water Resources, Budapest, Hungary, 2010. The hydrogeology of Ghana. *Hydrological Sciences Journal*, January .

Freeze, R. A. and Cherry, J. A., 1979. *Groundwater*. Prentice-Hall,(New Jersey): Englewood

Cliffs.

Geological Survey Department,(GSD), 2009. *Geological Map of Ghana 1: 000 000*. Accra:

GSD.

Geotomo Software, 2010. *Geoelectrical Imaging 2D & 3D Geotomo Software (RES2DINV ver. 3.59) manual*. Minden Heights, 11700 Gelugor(Penang): s.n.

Gill, H. E., 1969. *A Groundwater reconnaissance of the Republic of Ghana, with a description of geohydrologic provinces*. Washington: National government publication.

Gyau-Boakye, P., Kankam-Yeboah, K., Dapaah-Siakwan, S. and Darko, P. K., 2008.

Groundwater as vital resource for rural development: An example from Ghana. In: A. M. Segun Adelana, ed. *Applied groundwater studies in Africa* :Taylor & Francis, pp. 149-170.

Heath, R. C., 1987. *Basic Ground-Water Hydrology*, North Carolina: United States Geological Survey.

Hirdes, W., Senger, R. and Adjei, J., 1993. *Explanatory Notes for the Geological Map of Southwest Ghana*, Hannover: Geologisches Jahrbuch Reihe B, Band B 83.

Kankam-Yeboah, K., Dapaah-Siakwan, S., Nishigaki, M. and Komatsu, M., 2003. The hydrogeological setting of Ghana and the potential for underground dams. *Journal of the Faculty of Enviromental Science and Technology, Okayama University*, p. 39-52.

Kearey Philip, Michael Brooks and Ian Hill, 2002. *An Introduction to Geophysical Exploration*. third ed.:Blackwell Science Ltd.

Kempton, J. P. and Larson, D. R., 1997. *Geologic, Geophysical, and Hydrologic Investigations for a Supplemental Municipal Groundwater Supply, Danville, Illinois*, Houston,

TX 77073 United States of America: Baker Hughes INTEQ.

Key, R., 1992. An introduction to the crystalline basement of Africa. In : The hydrogeology of crystalline basement aquifers in Africa. *Geological Society Special Publication*. Kortatsi, B.,

Tay, C. and Hayford, E., 2008. Hydrogeochemical evaluation of groundwater in the

Lower Offin Basin of Ghana. *Environmental Geology*, Feb. Volume 53 (8). Lloyd,

2010. *global water scarcity, Risks and challenges for business*, London: Lloyd's

All rights reserved.

Loke, M. H., 1997. Electrical imaging surveys for environmental and engineering studies,

A practical guide to 2D and 3D survey, Short Training Course Lecture Note.. Loke, M. H.,

2000. *Electrical imaging surveys for environmental and engineering studies*,

A practical guide to 2-D and 3-D surveys. s.l.:s.n.

Loke, M. H., 2010. *Tutorial : 2-D and 3-D electrical imaging surveys*.

Lowrie, W., 2007. *Fundamentals of Geophysics*. Second Edition ed. Zürich :

Cambridge University Press.

Milsom, J., 2003. *Field Geophysics*. THIRD EDITION ed. The Atrium, Southern Gate,

Chichester: John Wiley & Sons Ltd.

Nationalgeographic, 2013. *nationalgeographic.com*. [Online] Available at:

http://education.nationalgeographic.com/education/encyclopedia/aquifer/?ar_a=1

[Accessed Mar 2013].

Ndlovu, S., 2011. Using low cost geophysical methods to locate high yielding groundwater

aquifers in the granite rock region of matabeleland south province of zimbabwe - a case

of gwatemba area. *Journal of Sustainable Development in Africa*, Volume Volume 13,

No.6, 2011, pp. 246-257.

Nelson, A. S., 2012. *Department of Earth and Environmental Sciences Tulane University*.

[Online]

Available at: <http://www.tulane.edu/~sanelson/geol111/index.html#Topics>

[Accessed 14 December 2012].

Nichols, G., 2009. *Sedimentology and stratigraphy*. second ed. Southern Gate, Chichester, West Sussex, PO19 8SQ: Blackwell Publishing.

Nicola, M. and Nick van de Giesen, 2005. Spatial Distribution of Groundwater Production and Development Potential in the Volta River basin of Ghana and Burkina Faso.

International Water Resources Association, June, Volume 30 Number 2, p. 239–249.

Obuobie, E. and Boubacar, B., December, 2010. *Groundwater in sub-Saharan Africa: Implications for food security and livelihoods*, International Water Management Institute (IWMI).

Owen, R. J., Gwavava, O. and Gwaze, P., 2005. Multi-electrode resistivity survey for groundwater exploration in the Harare greenstone belt, Zimbabwe. *Hydrogeology Journal*.

Ratnakumari, Y., Rai, S. N., Thiagarajan, S. and Kumar, D., 2012. 2D Electrical resistivity imaging for delineation of deeper aquifers in a part of the Chandrabhaga river basin,

Nagpur District, Maharashtra, India. *Current science*, January. Volume 102, NO. 1. Ravindran,

A. A., Ramanujam, N. and Somasundaram, P., 2012. Wenner array resistivity and sp logging for ground water exploration in sawerpuram teri deposits, thoothukudi district, tamil nadu, india. *Asian Research Publishing Network (ARPN)*. All rights reserved.,

OCTOBER. Volume VOL. 1, NO. 1.

Reynolds, J. M., 1997. *An introduction to applied and environmental geophysics*. Chichester: John Wiley and Sons Limited.

Sabet, A. M., 1975. Vertical Electrical Resistivity soundings to locate ground water resources: a feasibility study. *Virginia Water Resources Research Center, Virginia Polytechnic*

Institute and State University.

Sirhan, A., Hamidi, M. and Andrieux, P., 2011. Electrical resistivity tomography, An assessment tool for water resource:case study of Al-Arounbbasin, West bank, Palestine.

Asia Journal of Earth Sciences.

Tain District Assembly, 2006. <http://tain.ghanadistricts.gov.gh>. [Online]

Available at: <http://tain.ghanadistricts.gov.gh> [Accessed 2013].

Telford, W. M., Geldart, L. P. and Sheriff, R. E., 1990. *Applied geophysics*. Cambridg:
Cambridge university press.

Todd, D., 1980. *Groundwater Hydrology Groundwater Hydrology*. New York: John Wiley.

UNESCO, 2004. *Groundwater resources of the world and their use*. Paris, France:

United Nation Educational, Scientific and Cultural Organization.

UNESCO, WHO and UNEP, 1992, 1996. *Water quality assessments: A guide to the use of biota, sediments and water in environmental monitoring*. second ed. London SE1 8HN:

UNESCO, WHO and UNEP by E&FN Spon.

U. S. Environmental Protection Agency, 2011. *United States Environmental Protection Agency*.

<http://www.epa.gov> [Online] Available at:

http://www.epa.gov/esd/cmb/GeophysicsWebsite/pages/reference/methods/Surface_Geophysical_Methods/Electrical_Methods/Resistivity_Methods.htm [Accessed May 2013]

Vandas, S. J., Winte., T. C. and Battaglin, W. A., 2002. *Water and the environment (AGI Environmental Awareness Series)*. s.l.:American Geological Institute publications.

Van-Dycke, A., S. and Menyeh, A., 2013. Geo-Electrical Investigation Of Groundwater

Resources And Aquifer Characteristics In Some Small Communities In The Gushiegu And Karaga Districts Of Northern Ghana. *International journal of scientific & technology research*, March.2(3).

WHO, 2004. *Guidelines for Drinking-water Quality*, 20 Avenue Appia, 1211 Geneva 27, Switzerland: World Health Organization.

WHO, 2006. Groundwater and public health. In: G. Howard, *et al.* eds. *Protecting groundwater for health: Managing the quality of drinking-water sources*. London: IWA Publishing, UK.

WHO, 2010. *Guidelines for Drinking-water Quality*, Geneva 27, Switzerland: World Health Organization, 20 Avenue Appia.

WHO, 2010. *Water for health*, Geneva 27: World Health Organization.

WHYMAP ,BGR and UNESCO, 2008. *h map.or* . [Online]

Available at: http://www.whymap.org/whymap/EN/Home/whymap_node.html

[Accessed 17 Nov. 2012].

WRI of CSIR, 1993. *Groundwater assessment report on the Accra plains*, Accra: Unpublished .

Yankey, R. K., Akiti, T. T., Osae, S. R., Fianko J., Duncan, E. A.; Amartey, O. E., 2011.

The Hydrochemical Characteristics of Groundwater in the Tarkwa Mining Area, Ghana.

Research Journal of Environmental and Earth Sciences.

Zohdy, A. A. R. , Eaton G. P. and Mabey D. R., 1974. Application of surface geophysics to ground-water investigations. p. 11 6.

APPENDIX

Appendix A.1 The list and population of beneficiary communities in Tain District

No	Community	Geographic Position				Population (2010)	No. of BHs
		Lat.	Long				
1	Menji	7.92619	-2.39061	310	1		
2	Kwametenten	7.91164	-2.41819	621	1		
3	Debibi	7.89565	-2.54017	342	1		
4	Sekogor	7.89405	-2.5423	432	1		
5	Mempeasem No.1	7.86173	-2.50362	430	1		
6	Ehiamankyene No.2	7.87777	-2.21536	330	1		
7	Wiasekrom	7.94779	-2.28473	301	1		
8	Taiano-Banda Boase	8.00504	-2.14706	310	1		
9	Mmampehia	7.75945	-2.30665	340	1		
10	Samdew	7.72452	-2.38321	450	1		
11	Kuntuntadese	7.71016	-2.31187	401	1		
12	Kwadwokrom-Nkona	7.95307	-2.33541	320	1		
13	Bepoyease	7.73876	-2.21465	400	1		
14	Konkonti	7.62417	-2.45072	620	1		
15	Nnfodwo	7.60141	-2.4552	457	1		
16	Amangoase	7.57745	-2.39748	350	1		
17	Seikwa Sda Pri.	7.71466	-2.52564	350	1		
18	Kwadwokrom	7.80834	-2.42559	350	1		
19	Banda Ahenkro	8.16239	-2.35676	620	1		
20	Dorbor	8.09022	-2.51773	909	1		

Appendix A.2 Ranking points for drilling in beneficiary communities.

Geographic position							Ranked drilling		
		points	No	Community	Geologic settings	Lat.	Long	1 st	2 nd
1	Menji	7.92619	-2.39061	A80 105	Sandstone with some				siltstone of Tarkwaian formation.
	Menji		7.92619			-2.39061	B145	B90	Sandstone with some siltstone of Tarkwaian formation.
2	Kwametenten	7.91164	-2.41819	A130 A60	Sandstone with some				siltstone of Tarkwaian formation.
									Kwametenten 7.91164 - 2.41819 B40 B155 Sandstone with some siltstone of Tarkwaian

KNUST

formation

3	Debibi 7.89565	-2.54017	60	145	Argillitic/pelitic sediments of Birimian formation.	
4	Sekogor	7.89405	-2.5423	95	60	Argillitic/pelitic sediments of Birimian formation.
5	Mempeasem No.1	7.86173	-2.50362	170	30	Conglomerate and sandstone Tarkwain and Argillitic/pelitic sediments of Birimian formation.
6	Ehiamankyene No.2	7.87777	-2.21536	60	80	Argillitic/pelitic sediments of Birimian formation.
7	Wiasekrom	7.94779	-2.28473	80	115	Wacke sediments of Birimian formation.

8	Taiano-Banda Boase	8.00504	-2.14706	110	135	Argillitic/pelitic sediments of Birimian formation.
9	Mmampehia	7.75945	-2.30665	140	40	Argillitic/pelitic sediments of Birimian formation.
10	Samdew	7.72452	-2.38321	A30	A110	Argillitic/pelitic sediments of Birimian formation.
11	Kuntuntadease	7.71016	-2.31187	75	135	Wacke sediments of Birimian formation.
12	Kwadwokrom-Nkona	7.95307	-2.33541	120	75	Wacke sediments of Birimian formation.
13	Bepoyease	7.73876	-2.21465	115	150	Argillitic/pelitic sediments of Birimian formation.
14	Konkonti	7.62417	-2.45072	35	145	Argillitic/pelitic

KNUST

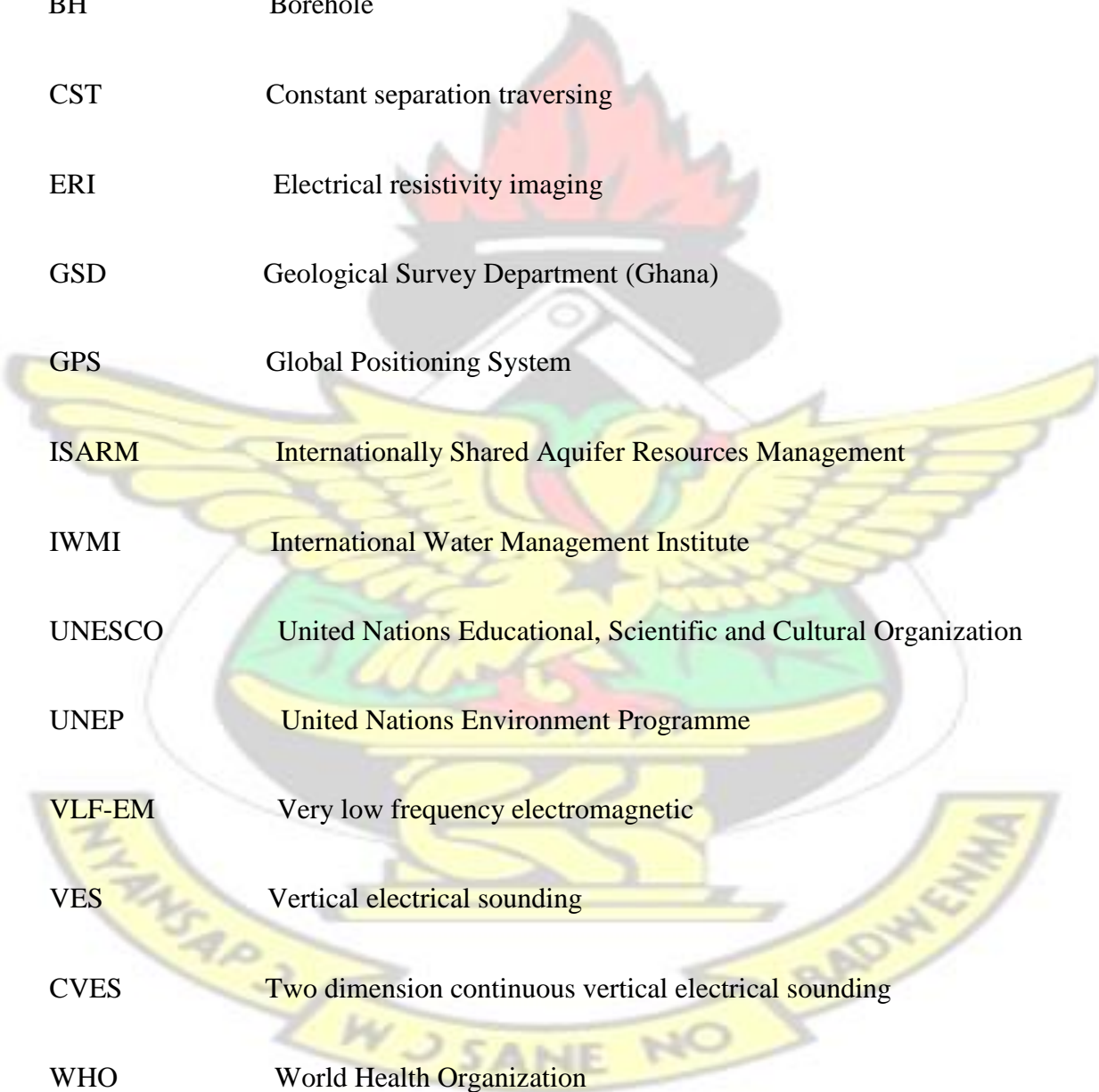
15	Nnfodwo	7.60141	-2.4552	45	112	Argillitic/pelitic	sediments of Birimian formation.
16	Amangoase	7.57745	-2.39748	100	120	Argillitic/pelitic	sediments of Birimian formation.
17	Seikwa	7.71466	-2.52564	140	95	Argillitic/pelitic	sediments of Birimian formation.
18	Kwadwokrom /Sulage	7.80834	-2.42559	95	60	Argillitic/pelitic	sediments of Birimian formation.
19	Banda Ahenkro	8.16239	-2.35676	150	45	Sandstone with some	siltstone of Tarkwaian formation.
20	Dorbor	8.09022	-2.51773	100	35	Argillitic/pelitic	

KNUST

sediments of Birimian
formation



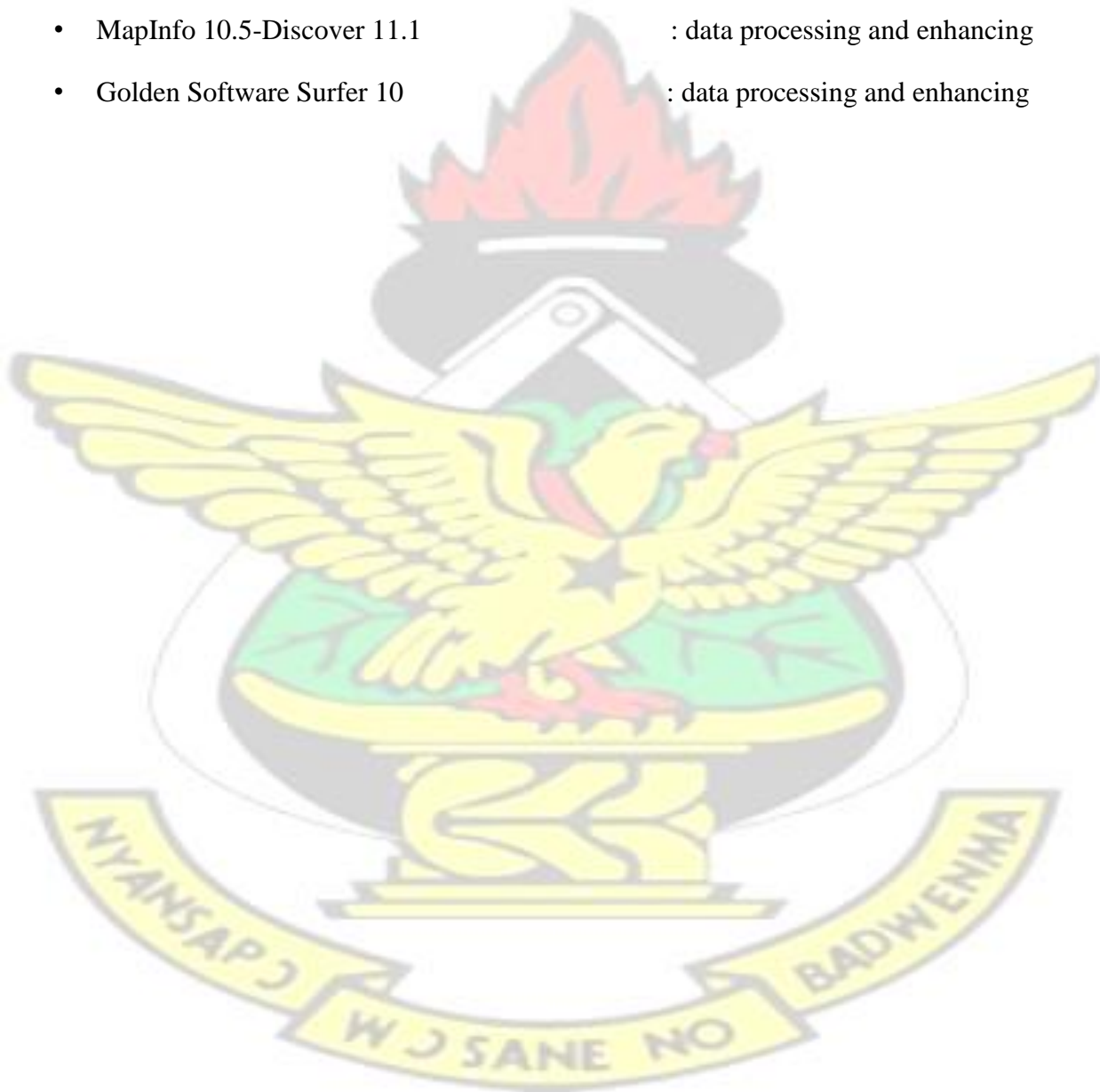
Appendix B.1 List of abbreviations



BGR	Bundesanstalt für Geowissenschaften und Rohstoffe
BGS	British Geological Survey
BH	Borehole
CST	Constant separation traversing
ERI	Electrical resistivity imaging
GSD	Geological Survey Department (Ghana)
GPS	Global Positioning System
ISARM	Internationally Shared Aquifer Resources Management
IWMI	International Water Management Institute
UNESCO	United Nations Educational, Scientific and Cultural Organization
UNEP	United Nations Environment Programme
VLF-EM	Very low frequency electromagnetic
VES	Vertical electrical sounding
CVES	Two dimension continuous vertical electrical sounding
WHO	World Health Organization

WHYMAP World-wide Hydrogeological Mapping and Assessment Programme
Appendix B.2 Used Softwares

- Microsoft office : typesetting and layout
- Geotomo Software (RES2DINV ver. 3.59.22) : data processing and enhancing
- Coral Draw X5 : graphics
- MapInfo 10.5-Discover 11.1 : data processing and enhancing
- Golden Software Surfer 10 : data processing and enhancing



KNUST

